

THESIS FOR THE DEGREE OF DOCTOR OF PHILOSOPHY

**Mass Transport Through Polymer Films:
The Importance of Interfaces and Compatibility**

SOFIE GÅRDEBJER



Department of Chemistry and Chemical Engineering

CHALMERS UNIVERSITY OF TECHNOLOGY

Göteborg, Sweden 2016

MASS TRANSPORT THROUGH POLYMER FILMS: THE IMPORTANCE OF INTERFACES AND COMPATIBILITY

SOFIE GÅRDEBJER

© SOFIE GÅRDEBJER, 2016
ISBN 978-91-7597-306-7

Doktorsavhandlingar vid Chalmers tekniska högskola
Ny serie nr 3987
ISSN 0346-718X

Division of Applied Chemistry
Department of Chemistry and Chemical Engineering
Chalmers University of Technology
SE-412 96 Gothenburg
Sweden
Telephone + 46 (0) 31-772 10 00

Cover:

A schematic image of a diffusion cell used for permeability measurements and a laminated film consisting of LDPE and EAA (positive ion image from TOF-SIMS of diamond ultramicrotomed film) with a suggested linear concentration decline.

Chalmers Reproservice
Gothenburg, Sweden 2016

Mass Transport through Polymer Films: The Importance of Interfaces and Compatibility

SOFIE GÅRDEBJER

Department of Chemistry and Chemical Engineering

Chalmers University of Technology

Gothenburg, Sweden

ABSTRACT

Different types of barriers are used in packaging to keep and protect products from the surrounding environment and are often essential for storing and transportation. Today, many barriers are made of different types of polymers, but since most polymers do not exhibit desired barrier properties on their own, combinations must be used. One way to combine materials is to create composites by adding a filler to a matrix material. Another way is to combine numerous layers to form laminates. When two materials are combined, interfaces are formed between these materials. These interfaces can exhibit other properties than those of the bulks. For example, a filler can induce crystallinity in a matrix material, which will decrease its barrier properties. It is therefore important to understand the impact of interfaces on barrier properties for the production of functional barriers.

The major focus of this project was to study the mass transport of water and carboxylic acids in composites and laminates, respectively. To increase the compatibility between the matrix and the filler in a composite material, several surface modifications were used. It was shown that good dispersion of the filler was important for the production of homogenous films, but also that a rod-like nano-filler can cause pores in a composite material, resulting in increased water permeability. A simple and straightforward method was suggested to predict the dispersability of a filler in a polymeric matrix. The transport of carboxylic acids was studied in laminates with varying numbers of layers. It was found that laminates resulted in stronger barrier properties than single-layered films, likely because of the ordering of chains close to the interface. The results obtained in this thesis will contribute to the production of functional barriers.

Keywords: *Polymer films, Cellulose, Surface modification, Interfaces, Compatibility, Barriers*

LIST OF PUBLICATIONS

This thesis is based on the following scientific papers, referred to by their roman numerals in the text. The papers are appended at the end of the thesis.

- Paper I.** **Controlling water permeability of biodegradable composite films of polylactide acid, cellulose and xyloglucan**
Sofie Gårdebjer, Anette Larsson, Caroline Löfgren, Anna Ström
Journal of Applied Polymer Science 2015, **132**, 41219
- Paper II.** **Solid-state NMR to quantify surface coverage and chain length of lactic acid modified cellulose nanocrystals, used as filler in biodegradable composites**
Sofie Gårdebjer, Anna Bergstrand, Alexander Idström, Camilla Börstell, Stefan Naana, Lars Nordstierna, Anette Larsson
Composite Science and Technology 2015, **107**, 1-9
- Paper III.** **A mechanistic approach to explain the relation between increased dispersion of surface modified cellulose nanocrystals and final porosity in biodegradable films**
Sofie Gårdebjer, Anna Bergstrand, Anette Larsson
European Polymer Journal 2014, **57**, 160-168
- Paper IV.** **Using Hansen Solubility Parameters to predict dispersion of surface modified cellulose nanocrystals in hydrophobic polymers**
Sofie Gårdebjer, Martin Andersson, Jonas Engström, Per Restorp, Michael Persson, Anette Larsson
Accepted in Polymer Chemistry, 2016
- Paper V.** **The impact of interfaces in laminates for transport of carboxylic acids**
Sofie Gårdebjer, Tobias Gebäck, Thorbjörn Andersson, Emiliano Fratini, Piero Baglioni, Romain Bordes, Anna Viridén, Mark Nicholas, Niklas Lorén, Anette Larsson
Submitted

CONTRIBUTION REPORT

- Paper I.** Shared responsibility for the experimental outline and writing the manuscript with Anna Ström. Responsible for the main part of the experimental work.
- Paper II.** Performed experimental work with two MSc students. Shared supervision of the students with Anna Bergstrand. Responsible for writing the manuscript, except for the part covering solid-state NMR.
- Paper III.** Responsible for the main part of the experimental work. Responsible for interpretation of results and writing the manuscript with input from the co-authors.
- Paper IV.** Performed experimental work with an MSc student under my supervision. Responsible for interpretation of data and writing the manuscript with input from the co-authors.
- Paper V.** Responsible for the experimental work, except SAXS and WAXD. Responsible for writing the manuscript with input from the co-authors.

ABBREVIATIONS AND ACRONYMS

AFM	Atomic Force Microscopy
CNC	Cellulose Nanocrystals
DMA	Dynamic Mechanical Analysis
DSC	Differential Scanning Calorimetry
EAA	Ethylene Acrylic Acid
FT-IR	Fourier-Transform Infrared Spectroscopy
HSP	Hansen Solubility Parameters
LDPE	Low-Density Polyethylene
MCC	Microcrystalline Cellulose
mod-CNC	Surface-Modified Cellulose Nanocrystals
PEG	Poly(Ethylene Glycol)
PHB	Poly(3-Hydroxybutyrate)
PLA	Poly(lactide Acid)
PLGA	Poly(lactide-co-glycolide acid)
QCM	Quartz Crystal Microbalance-
RH	Relative Humidity
SAXS	Small Angle X-ray Scattering
SEC	Size Exclusion Chromatography
TOF-SIMS	Time-of-flight secondary ion mass spectrometry
WAXD	Wide-Angle X-ray Diffraction
XG	Xyloglucan

TABLE OF CONTENTS

INTRODUCTION.....	1
POLYMERS AS BARRIERS	3
2.1. Biodegradable Composites as Barriers.....	5
2.2. Laminates as Barriers.....	6
2.3. Transcrystalline Layers	7
INTERFACES AND COMPATIBILITY	9
3.1. Thermodynamic Models	10
3.2. Interfaces and Compatibility Between Polymers	12
3.2.1. <i>Interfaces in Composites</i>	12
3.2.2. <i>Interfaces in Laminates</i>	15
3.3. Solubility Parameters	17
MASS TRANSPORT IN POLYMER FILMS.....	19
4.1. Introduction to Mass Transport.....	19
4.1.1. <i>Measurements of Mass Transport in Films</i>	20
4.2. Mass Transport in Composites.....	23
4.3. Mass Transport in Laminates.....	25
EXPERIMENTAL OVERVIEW.....	27
OUTCOME OF RESEARCH.....	31
6.1. Mass Transport of Water in Composites.....	31
6.1.1. <i>Surface-Modified Cellulose via Adsorption</i>	31
6.1.2. <i>Chemical Surface-Modification of Cellulose</i>	35
6.1.3. <i>Prediction of Dispersability of Nano-Fillers in Polymers</i>	42
6.2 Mass Transport of Carboxylic Acids in Laminates.....	46
IMPORTANCE OF RESEARCH FOR INDUSTRIAL APPLICATIONS	51
CONCLUSIONS AND FUTURE OUTLOOK.....	53
ACKNOWLEDGMENTS	55
REFERENCES.....	57

INTRODUCTION

A barrier material protects a product from the environment and/or vice versa, and needs to prevent the transport of liquids and gases in both directions. Polymers can be used to produce films with barrier properties and different plastics are commonly used in packaging industry. These plastics are often fossil-based, but with increasing awareness of the environmental impact of these materials, biodegradable polymers have become more competitive on the market [1, 2]. Mass transport (or permeability) of a substance through a polymeric film depends on its diffusivity and solubility in the material [3, 4]. These properties depend in turn on factors such as chain packing and side group complexity, polarity, crystallinity, fillers, and plasticizers [3, 5].

Polymers do not exhibit the same barrier properties as more traditional materials such as glass or metal. Therefore, they are often combined with other polymers (or materials) to create functional barrier materials. One way to combine different materials is to create composites. A composite can consist of a matrix and a filler, often considered impermeable, that is used to enhance the properties of the matrix. In theory, this should result in improved barrier properties [6, 7]. One filler that has gained much attention in the last 20 to 30 years is cellulose [8-17]. Cellulose is the most abundant polymer on earth and a promising candidate for the production of totally biodegradable composites. However, due to large differences in surface chemistry, cellulose is incompatible with most plastics [11-13, 15-17], resulting in poor adhesion, decreased mechanical properties, and in some cases increased permeability of the final composite. To overcome this problem, the surface of cellulose may be modified to increase compatibility. The properties of two polymers can also be combined in layered structures—laminates—of different layers with different properties. For example, one layer may be a good oxygen barrier, while another is a good moisture barrier. Adding a filler or laminating different polymers may affect the diffusivity and/or the solubility of the permeant and hence result in changed permeability.

To develop highly efficient and economically viable barriers, it is important to understand the relationship between compatibility, adhesion, morphology, transport properties, and interfaces. By combining two or more materials, interfaces are created where the two different materials meet. In a composite material these interfaces are formed between the filler and the matrix and in a laminate the interfaces are formed between the layers. A major goal of this thesis was to study and modify these interfaces for composites and laminates and then measure the permeability of various

Introduction

permeants. Another major focus was to understand and explain the formation of the interfaces and the final microstructure of the produced films.

The major goals of this thesis were to:

- Study water permeability for composites upon addition of unmodified and surface-modified cellulose fillers.
- Study the permeability of carboxylic acids through laminates with various numbers of layers.

Chapter 2 gives a background of polymers used as barriers and Chapter 3 discusses interfaces and the importance of compatibility between two materials. Chapter 4 introduces mass transport properties over composites and laminates. Chapter 5 gives an overview of the experimental work and Chapter 6 concludes with the major finding of this work. Finally, Chapter 7 suggests how these findings could be used in future industrial applications.

This thesis contributes to studies undertaken at the VINN Excellence Centre SuMo BioMaterials (Supramolecular Biomaterials – Structure Dynamics and Properties), a joint effort of academic and industrial partners, and it focuses mainly on deepening our understanding of mass transport across barriers. These properties were also correlated with the microstructures of produced barrier materials, and this has improved our knowledge of material design.

POLYMERS AS BARRIERS

Packaging is necessary for transporting and storing products while also providing a platform to inform consumers about the contents. Packaging and barrier materials aim to protect a product from the surrounding environment and need to prevent the transport of liquids and gases in both directions. For example, it is important that the barrier shield against oxygen to avoid oxidation and/or mold in the product. It is also important that liquids do not enter or leave the packaging. Different types of barriers and packaging have been used as long as humankind has existed. Hunters and gatherers constructed devices of leaves, animal skin, or wood to carry their belongings and preserve food [18]. Woven grass baskets and clay pots were used to store dry foods and liquids. Glass, paper, and metals are all examples of materials with a long and continuing history of use as barriers. Glass-making is believed to be more than 9000 years old and its production was industrialized in Egypt 1500 BC [18]. The mixture of limestone, soda, sand, and silica has remained more or less the same, although molding techniques have developed. Paper production was initiated in China in the first or second century BC and introduced in England in 1310 AD. Tin plating was discovered in Bohemia around 1200 AD, and metal packaging became important in Europe in 1809 when Napoleon Bonaparte offered 12 000 francs to anyone who could preserve food for his army. A Parisian chef discovered how to preserve food in tin. Aluminum had already been extracted from bauxite iron by 1825, but it took until 1959 for the first aluminum can to enter the market. Aluminum is now commonly used in packaging because of its high barrier properties and light weight[19, 20].

Plastic, discovered in the 19th century [21], is a newer barrier material than glass, paper, and metal, although no plastics were practical to use as barriers until the 20th century. Polyethylene, discovered in the 1930s [21, 22], was one of the first plastics used for food packaging [23]. Polyethylene is a fossil-based thermoplastic available as high-density polyethylene, low-density polyethylene (LDPE), and linear low-density polyethylene. LDPE is a good moisture barrier, but a poor oxygen barrier [23]. Therefore, LDPE is often combined via co-extrusion with other plastics or materials to create an improved barrier. Figure 2.1a shows an example of a laminated film consisting of two materials, similar to one of the laminates studied in this thesis.

Polymers as Barriers

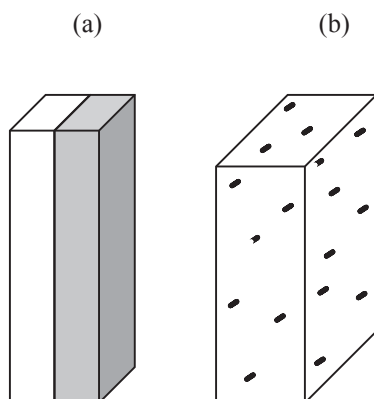


Figure 2.1. Schematic images of (a) a laminate and (b) a composite consisting of a matrix and a filler.

There are, however, problems connected to fossil-based plastics related to increased greenhouse gases and their environmental impact. Fossil-based plastics can take more than 100 years to degrade, and plastics pollute and interfere with nature and sea life. In recent years, interest in biodegradable polymers has increased [1, 2]. Examples of such polymers are polylactide acid (PLA), poly(lactide-co-glycolide acid) (PLGA) and poly(3-hydroxybutyrate) (PHB), which can be produced from plants or bacteria [24, 25]. However, biodegradable polymers are still more expensive than fossil-based polymers such as LDPE, and their barrier properties are not as good. There is also controversy about whether arable land should be used for food production or biodegradable plastics [26]. A solution to these problems, which also has economic benefits, is to create composites using a more abundant polymer as a filler (Figure 2.1b). Incorporating cellulose in biodegradable polymers has been widely studied and will be discussed in section 2.1. The overall goal of using a filler in a composite is often to improve the material's mechanical, thermal, and barrier properties.

2.1. Biodegradable Composites as Barriers

There is much interest in using biodegradable materials such as PLA (Figure 2.2) in applications that require resistance to moisture and water, i.e. packaging, agricultural mulch films, or biomedical devices [27-29]. PLA is a thermoplastic polymer that can be produced annually, and high molecular-mass PLA has been shown to have similar mechanical and barrier properties to polystyrene [30]. PLA has a glass transition temperature from 50°C to 80°C and a melting point from 130°C to 180°C depending on the nature of the polymer [30]. Its relatively low softening temperature has propelled efforts to incorporate different types of cellulose and to produce composites to improve thermal stability [11, 31]. Another advantage of incorporating a filler is to improve barrier properties by increased tortuosity path. A permeant needs to travel around the impermeable filler instead of directly through the matrix material, resulting in decreased permeability [6]. Incorporating cellulose in a PLA matrix has also been shown to induce crystallinity in the matrix [31-35]. Because crystalline parts are considered impermeable to smaller molecules, the barrier properties of such a matrix would be expected to increase.

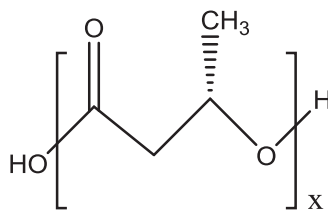


Figure 2.2. Chemical structure of the monomer of PLA.

For example, Oksman and co-workers have shown that microcrystalline cellulose as well as wood fibers can function as nucleating agents in a PLA matrix [31]. Other studies have shown similar results for cellulose nanocrystals (CNC) [33-35]. CNC have gained interest in recent years due to their defined structure and high surface area [24, 36]. The addition of these nano-fillers has also been shown to increase mechanical properties of final composite films [33, 34, 37-40]. In these cases, the surface of CNC has often been modified in order to increase the compatibility with the polymer matrix. Good compatibility between the matrix and filler has been shown to be important to receive a good dispersion of the fillers and hence a homogeneous material with increased barrier properties [12-14, 16, 34, 35]. For example, Sanchez-Garcia and co-workers showed a reduction of both water and oxygen permeability of up to 5 wt% in well-dispersed CNC in a polymer matrix [35]. However, the opposite has also been found. Fortunati and co-workers prepared films of PLA combined with CNC and surface-modified CNC by solvent casting. The CNC was modified with an acid phosphate ester of ethoxylated nonylphenol and the addition of 1 wt% of the modified CNC resulted in a 34% decrease of the water vapor permeability, while 5 wt% resulted in the same water vapor permeability as the pure material [41]. Pereda

and co-workers showed that water vapor permeability increased in casein films with up to 3 wt% added CNC [39]. This was explained by cracks and bubble formation induced in the structure upon addition of the filler.

2.2. Laminates as Barriers

For a barrier material to function properly, it needs to provide good protection against liquid, moisture, and gases. It also needs rigidity for transport and protection of food. Therefore, barrier films in food packaging often consist of laminates in which each layer has different properties. Polypropylene and polyethylene are polymers with good resistance to liquid and moisture, while polyamide and ethylene vinyl alcohol are examples of good oxygen barriers [23, 42]. The outside of the packaging is often made of cardboard, which gives rigidity but also provides useful information to the consumer. Laminates are often produced via co-extrusion with two or more plastic granules heated and melted separately. The melts are thereafter brought together in a single film.



Figure 2.3. Chemical structures of the monomers for (a) LDPE and (b) EAA.

Polyethylene is one of the most generically used polymers in food packaging because of its relatively low cost and high barrier properties to water [43]. Figure 2.3a shows the ethylene monomer of LDPE, which is a thermoplastic polymer with a glass transition temperature well below room temperature and a melting temperature in the range of 105°C to 118°C [44]. LDPE is branched and usually has a crystallinity in the range of 45% to 60%. Ethylene acrylic acid (EAA) (monomer shown in Figure 2.3b) is a copolymer of ethylene and acrylic acid, and is usually more amorphous than LDPE. The addition of acrylic acid groups contributes to increased polarity and

toughness, and these groups can also orient and interact with metals such as aluminum. The copolymer is therefore suitable for a large range of industrial applications [45, 46] since introduction of metals e.g. aluminum in a laminate is commonly used to increase its barrier properties. The use of a copolymer with increased adhesion to the metal has been shown to be important in food packaging since there is a risk of delamination if fatty acids enter the interface between two less adhesive layers such as LDPE and aluminum [47].

2.3. Transcrystalline Layers

Transcrystalline layers can form in both composites and laminates in a heterogeneous nucleation-controlled process occurring in a semi-crystalline polymer in contact with another material [48, 49]. Since crystalline parts of a material are considered impermeable, the formation of these layers could be an advantage for barriers. A presumption of the formation of a transcrystalline layer is that a high density of active nuclei is formed on one of the substrate surface [50]. The layers are then forced to grow perpendicular to the surface, due to the close packed nuclei [50, 51]. Transcrystalline layers affect the interfacial adhesion and the mechanical properties of the bulk [51, 52]. For example, Huan and co-workers induced transcrystalline layers in PLA by the addition of ramie fibers with poly-(ethylene glycol) (PEG) added as a crystallization accelerator, which improved the chain mobility of PLA [53]. It was shown that the addition of up to 10 wt% of PEG chains increased the interfacial shear strength.

Broseta and co-workers showed that low molecular weight chains and high polydispersity have impact on the interface and the formation of transcrystalline layers in laminates [54]. Polymers with high polydispersity and shorter chains result in a thicker interface. This is explained by the advantageous entropy gained in the system by excluding the longer chains from the interface [54]. Even between two immiscible polymers, a transcrystalline layer can form close to the interface as a result of high polydispersity and the diffusion of shorter chains into the interface [55]. McEvoy and Krause showed that transcrystalline layers less than 5 μm wide were formed between polyethylene and a copolymer of EAA that consisted of 3 wt% acrylic acid groups [55], which is a similar material to the laminates used in this thesis. Again, this was explained by the diffusion of shorter chains. The formation of transcrystalline layers are expected to decrease the permeability of both composite and laminates

INTERFACES AND COMPATIBILITY

Interfaces, present in pure and in multicomponent materials, are those microstructural regions that separate two phases [56]. The interface depends on the property under consideration and it may range from less than a nanometer up to more than a millimeter in thickness [57, 58]. Pure materials form an interface between the liquid or solid phase and the vapor phase and are usually referred to as the *liquid/solid-vapor interface* or the *liquid/solid surface*. Interfaces between two solid materials are referred to as *solid-solid interfaces*, *interphase interfaces*, or *interphase boundaries*. An additional term is *grain interface*, used for two phases with identical structure and composition, and differing only in crystallographic orientation [59]. In this thesis, the word *interface* will refer to the area formed between two different polymers in the solid state. The materials these polymers form are either composites, with interfaces between the matrix and the filler, or laminates with interfaces between the different layers.

Polymeric interfaces have two types of interfaces: the first, with two miscible polymers, is also referred to as a symmetric interface [60]. In this case, the kinetics of the polymers determine the structure of the interface, which means that it is important to understand and control the dynamics of diffusing chains, the annealing time, and the molecular weight of the polymer chains. The width of the interface for two miscible polymers evolves over time and involves the mechanisms of polymer interdiffusion, explained in the literature by the theories of reptation and Rouse-type [61, 62]. The second type of interface, formed between two polymers that are immiscible, is also referred to as an asymmetric interface. This type of interface is more common when there is a large difference in glass transition temperature between the two polymers [60]. The typical width of interfaces formed between two polymers is in the range of 1 to 50 nm, depending on the compatibility of the polymers [63]. In practice, many polymers are immiscible or only partly miscible.

Interfacial energy is denoted γ (typically in mJ/m^2) and is defined as the reversible work required for creating a unit area of surface, at a constant temperature, volume (or pressure), and chemical potential. The interface is usually not perfectly sharp, for example in an interface between liquid and vapor there will be a transition region with differing densities [56, 64]. Interfacial energy is a thermodynamic property that can be calculated from statistical thermodynamic theories. It may be important to consider, since it affects the morphology of a multiphase polymer system. In general,

interfacial tension between two polymers decreases linearly with temperature and increases with the increasing molecular weight of the polymer chains [65].

3.1. Thermodynamic Models

Thermodynamic models can be used to explain the formation of an interface and the compatibility between two polymers. This section is aimed to give an overview of the basic thermodynamics of the miscibility of two polymers. Most theories for miscibility of polymers were developed from Flory-Hugging mean-field theory, which was independently developed by Flory [66] and Huggins [67, 68] in 1942. The theory is based on a model in which the polymers are placed within a lattice and the volume is considered constant during mixing. The term *mean-field* refers to the consideration of only average interactions. The thermodynamic expression for mixing two components is defined by the free energy change of mixing:

$$\Delta G_{mix} = \Delta H_{mix} - T\Delta S_{mix} \quad (1)$$

where T is the absolute temperature and ΔH_{mix} and ΔS_{mix} are the enthalpy and entropy change of mixing. If $\Delta G_{mix} < 0$ it is possible to mix the components in the system, but if $\Delta G_{mix} > 0$, the two polymers are immiscible. For a binary system in the Flory-Huggins mean-field theory, the free energy can be expressed as:

$$\Delta G_{mix} = k_B T \left[\frac{\phi_1}{n_1} \ln \phi_{1_1} + \frac{\phi_2}{n_2} \ln \phi_2 + \chi \phi_1 \phi_2 \right] \quad (2)$$

where ϕ_1 and ϕ_2 are the volume fractions, n_1 and n_2 are the degrees of polymerization (e.g. the number average molecular weight divided by the monomer molecular weight), and χ is the Flory-Huggins interaction parameter. The first two terms in Equation 2 relate to the entropy of mixing and the third to the enthalpy of mixing. Most polymer blends are immiscible or just partly miscible and form multiphase systems. The entropy of mixing, ΔS_{mix} , is small for polymers because of its high molecular weight, and it approaches zero with increasing molecular weight [63, 69]. Therefore, mixing two polymers will depend mainly on the enthalpy of mixing, ΔH_{mix} , according to Equation 1. However, in most cases the interactions between the different chains are relatively weak and often show a positive ΔH_{mix} , resulting in phase-separation of the polymers. However, if there is a favorable energetic interaction between segments of the two polymers (for example dipole-dipole, ion or hydrogen bonding) it is possible to have a negative ΔH_{mix} , which then results in a negative ΔG_{mix} and hence a miscible interface [58]. Additionally, according to Equation 2, a negative Flory-Huggins parameter χ should also result in miscibility, but for polymers miscibility is achieved when $\chi < \chi_{cr}$, where χ_{cr} is defined as:

Interfaces and Compatibility

$$\chi_{cr} = \frac{1}{2} \left[\frac{1}{\sqrt{n_1}} + \frac{1}{\sqrt{n_2}} \right]^2 \quad (3)$$

It is also possible to calculate an analytical solution for the volume fraction profile of an interface using thermodynamic properties. The most basic theory uses mean-field theories. Fluctuations, excluded volumes and finite size effects are not taken into account:

$$\phi(z) = \frac{1}{2} \left[1 + \tanh \left(\frac{2z}{a_l} \right) \right] \quad (4)$$

where ϕ is the volume fraction, z is the coordinate perpendicular to the interface, and a_l is the interfacial width. In the case of immiscible polymers, the interfacial length can be calculated according to Equation 5 if the interaction parameter χ is known:

$$a_l = \frac{2b}{\sqrt{\chi \cdot c}} \quad (5)$$

where b is the Kuhn segment length, i.e. a real polymer chain is considered as a collection of N Kuhn segments which are freely joined with each other, and $c=6$ if $a_l \leq R_g$ and $c=9$ if $a_l \geq R_g$ which has been confirmed by several neutron reflectivity experiments [70, 71]. However, the theory does not take into account surface roughness, chain end effects, fluctuations at the interface, or molecular weight distribution, which may be important for interfacial formation.

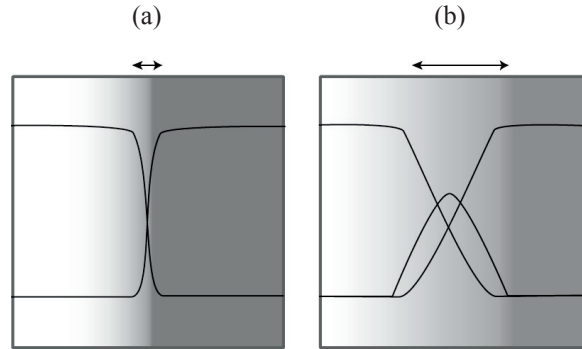


Figure 3.1. Schematic drawing of (a) an immiscible interface and (b) a miscible interface. The concentration profile is shown as lines in the figure, and in the second case a compatibilizer has been added which results in a wider interface.

Figure 3.1a shows two immiscible polymers with a sharp interface formed in the Angstrom-nanometer range. A prefabricated interfacial agent (as shown in Figure 3.1b) may be used to mix two immiscible polymers or to reduce interfacial tension. This agent, often called a compatibilizer, can consist of a di-block copolymer in which each block is miscible in either polymer. The modification of the interfacial properties will lead to lower interfacial tension [58], resulting in improved adhesion and increased compatibility between the polymers [55, 72]. Tri-block copolymers can also be used to form hairpins between two polymers, and random copolymers can form several connections between two polymers [73].

3.2. Interfaces and Compatibility Between Polymers

Although most polymers are immiscible or only partly miscible, there is great interest in understanding compatibility between two polymers. The following sections give an introduction to interfaces in composites and laminates and also introduce the experimental work undertaken for this thesis.

3.2.1. Interfaces in Composites

Composites consist of at least two different constituents: a matrix and a filler. The filler is used to improve the properties of the matrix [51, 74]. Numerous interfaces are formed between the matrix and the filler. Adhesion between the filler and the matrix affects stress transfer in the material, which is important for obtaining good mechanical properties such as high strength [51, 75]. Given that the filler functions as reinforcement, strong adhesion between the matrix and filler creates a composite with high strength and stiffness, but that is brittle and cracks easily. Weak adhesion reduces the efficiency of stress transfer from the matrix to the filler, resulting in lower tensile strength and stiffness. A crack easily propagates along the filler-matrix interface if the interface is weak, which can result in debonding and/or pull-out of the filler [51].

In Papers I–IV we studied the importance of adhesion and compatibility between matrix and filler using different types of cellulose at both the micro- and nanoscale levels and different types of surface modifications. The much discussed poor adhesion between cellulose and many polymers [11-13, 15-17], is usually explained by the difference in hydrophobicity between the materials. As have many others, we modified the surface of cellulose in different ways. In the study reported in Paper I, varying amounts of the hemicellulose xyloglucan were adsorbed to the surface of microcrystalline cellulose by simply mixing microcrystalline cellulose and

hemicellulose in a water suspension overnight, then freeze-drying and extruding with PLA (Figure 3.2a). This study was based on results from Raj and co-workers, who showed that adhesion between xyloglucan and PLA was stronger than adhesion between cellulose and PLA [15].

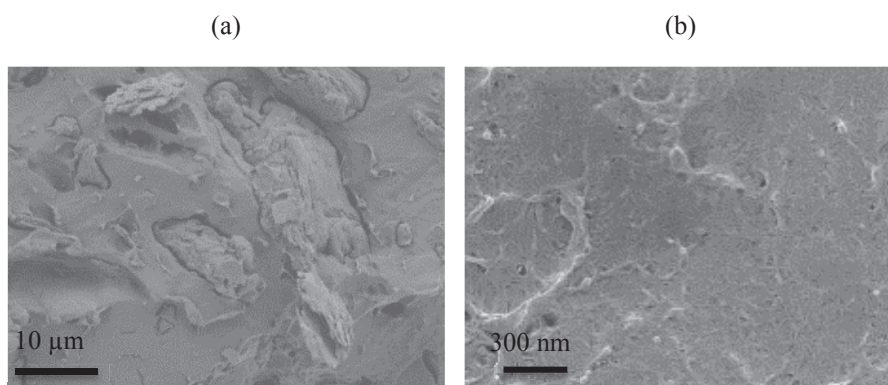


Figure 3.2. SEM images of composites consisting of (a) PLA and microcrystalline cellulose [76] and (b) LDPE and cellulose nanocrystals. Note that the scale bars are different in the two images.

In Papers II, III, and IV, CNC was dispersed into different hydrophobic polymers to create nanocomposites (see example in Figure 3.2b). The term nanocomposite is widely used to describe a broad range of materials, with at least one of the components requiring a sub-micron dimension scale [77]. Nano-fillers with a high aspect ratio give other mechanical and rheological properties to the composites than larger fillers do [78, 79]. However, for improved properties in the film it is important that the nano-filler is well dispersed in the matrix. A method often used to produce these films is solvent casting, which use a solvent to dissolve the polymer. These solvents are usually not appropriate for the more hydrophilic cellulose, and aggregation of CNC can occur already in the organic solvent [33, 80]; these aggregates will remain in the film. One option to make CNC more compatible with the polymer matrix is to modify the surface of CNC with hydrophobic chains. The effects of the surface modification of cellulose have been widely studied [13, 14, 16, 33, 35, 81-86]. Figure 3.3 shows images from polarized microscopy where the black areas represent totally amorphous parts and white parts represent crystalline parts [80]. The pure PLA film in Figure 3.3a is totally amorphous, while the addition of 10 wt% unmodified CNC resulted in an inhomogeneous material with large aggregates

(shown with green circles in Figure 3.3b). After surface modification of CNC, the film shows a more homogeneous distribution of the cellulose (Figure 3.3c).

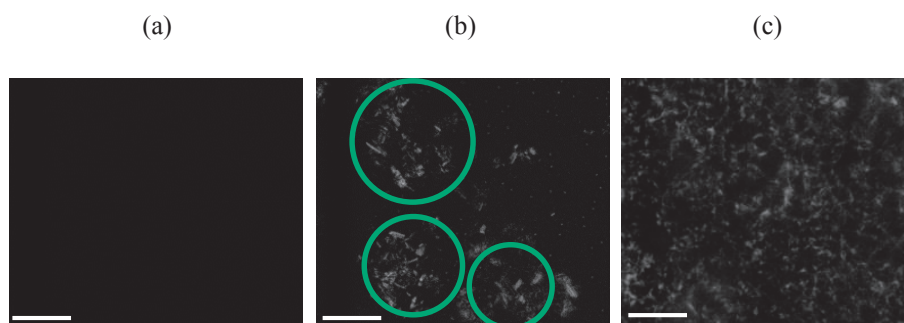


Figure 3.3. Polarized light microscopy images of (a) PLA and nanocomposite films with (b) 10 wt% CNC and (c) 10 wt% surface modified CNC. Black parts are totally amorphous while white parts are crystalline and mainly correspond to CNC. The white scale bar in each image represents 100 μm .

Figures 3.4a-b shows the reactions used for surface modification of CNC in this thesis. In the first case, a ring opening of L-lactide was performed and the successful modification was characterized by an extensive solid-state NMR study, the results of which were reported in Paper II. Nanocomposites were produced, investigated, and reported in Paper III, where we also suggest a mechanism for pore formation observed in the solvent-casted films. In the second case, a chlorohydrin was attached to the surface of the CNC. The length of carbon chains on the chlorohydrin differed and these modified CNC were used to develop a method to predict of dispersability of CNC in a polymer in the study reported in Paper IV.

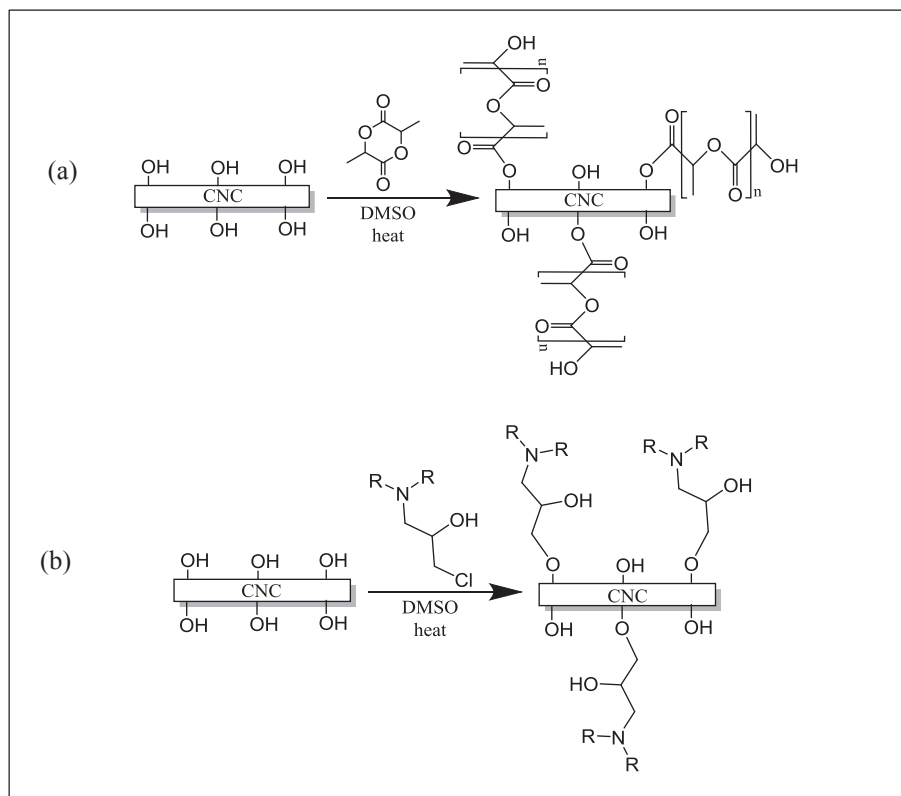


Figure 3.4. Reactions for surface modifications of CNC, in (a) *L*-lactide via a ring-opening polymerization and (b) chlorohydrins with varying carbon chain lengths (*R* is equal to 6 or an average of 17 carbons). Sulfate ester groups on CNC surfaces are not shown.

3.2.2. Interfaces in Laminates

Many polymers are immiscible or partly miscible and much effort has been spent on understanding how to compatibilize two immiscible polymers [55, 57, 58, 65]. Many studies have investigated the interface using different scattering or reflectometry techniques [70, 71, 87] with resolutions reaching as low as the nanometer scale. Since most polymers are immiscible, interfacial thicknesses are often in the range of Å-nm [60, 70, 87, 88]. It is also important that laminated have good mechanical strength, achievable through compatibilizers.

In the packaging industry, it is well-known that adhesion between LDPE and aluminum is poor [89]. It can however be improved by partially oxidizing LDPE by,

for example, using corona discharge treatment [89, 90]. Another way to improve adhesion is to use a polymer with polar groups, for example EAA, which can interact with the aluminum through its polar groups to increase adhesion [45, 90]. Another frequent problem is that certain food components such as oils and fats can be dissolved in the polymers. These components can then enter the interface, lowering the interfacial energy causing delamination [47, 91, 92]. Olafsson and co-workers showed that unsaturated fatty acids caused delamination of LDPE/aluminum foil within a few days [91]. In a similar study, they showed that acetic acid also caused delamination of LDPE and aluminum [47]. Ortiz and co-workers measured accumulations of volatile and semi-volatile compounds especially between aluminum and a polyester film [93]. They showed such compounds migrated mainly to the aluminum surface, resulting in decreased adhesion. Adhesion has also been directly correlated to the interfacial width of both immiscible and miscible glassy polymers [60]. In that study, interfacial width was determined by neutron reflectivity and the fracture toughness of the laminate was measured.

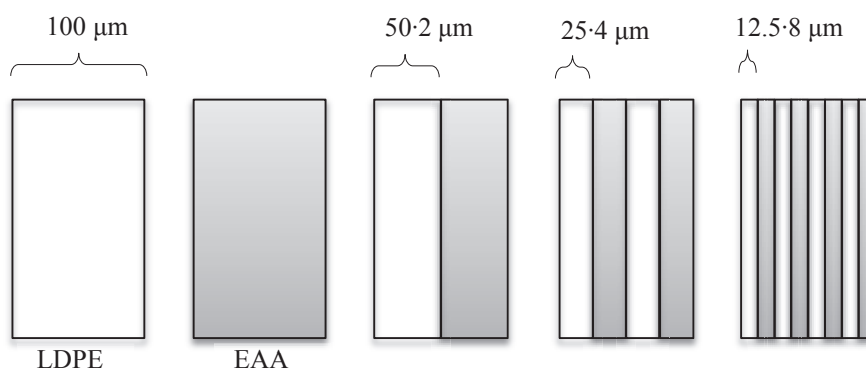


Figure 3.5. Schematic image of two pure films and 2-, 4-, and 8-layered laminates investigated in this thesis. Total thickness of all films were 100 μm .

Similar to that study, the laminates studied for this thesis consisted of two similar polymers. Two of the films were pure materials consisting either of LDPE or EAA. The other films consisted of layers of LDPE and EAA, and 2-, 4- and 8-layered films were investigated. Figure 3.5 shows a schematic image of the different films, where the total thicknesses of all films were 100 μm .

3.3. Solubility Parameters

Solubility parameters have been used for many years to calculate and predict the solubility of a polymer in different solvents. In recent years, attempts have been made to predict the colloidal behavior of nanoparticles in solvents [94, 95]. This was also the case in our study in which CNC was surface-modified with substituents of varying carbon chain lengths. The term solubility parameters was first used by Hildebrand and Scott and is defined as the square root of the cohesive energy density [96]:

$$\delta_T = \sqrt{\frac{E_{coh}}{V}} \quad (6)$$

where V is the molar volume of the solvent and E_{coh} is the energy of vaporization. As discussed in section 3.1, free energy must be smaller than 0 for a system to mix. Following the approach of Flory-Huggins [97], the enthalpy of mixing can be expressed as:

$$\Delta H_{mix} = k_B T \chi \phi_1 \phi_2 / v_0 \quad (7)$$

where ϕ_1 and ϕ_2 are the volume fractions, v_0 is the molar volume, and χ is the Flory-Huggins interaction parameter. For small molecules, the enthalpy of mixing can be described as in Equation 2 or by using the Hildebrand-Scratchard expression:

$$\Delta H_{mix} = (\delta_{T,A} - \delta_{T,B})^2 \phi_1 \phi_2 \quad (8)$$

where $\delta_{T,A}$ and $\delta_{T,B}$ are the Hildebrand solubility parameters of the solute and the solvent, respectively. Combining Equation 7 and 8 gives:

$$\chi = \frac{v_0}{k_B T} (\delta_{T,A} - \delta_{T,B})^2 \quad (9)$$

where it can be seen that the Flory-Huggins parameter is always positive and the solubility parameters for species A and B should be as close as possible for the system to mix. Even though Hildebrand solubility parameters are well documented for many systems, they cannot themselves describe a system since they only cover the London interactions between the compounds. However, most systems include (atomic) dispersion forces, (molecular) permanent dipole-permanent dipole forces, and (molecular) hydrogen bonding (electron exchange) [98]. These factors are all described by the Hansen solubility parameters (HSP):

$$\delta_{TOT}^2 = \delta_D^2 + \delta_P^2 + \delta_H^2 \quad (10)$$

where δ_D , δ_P , and δ_H represent dispersion, polar, and hydrogen-bonding interactions, respectively. Materials with similar HSP have high affinity for each other. In recent

Interfaces and Compatibility

years it has become interesting to measure the dispersability of nanoparticles in solvents. In these cases, the goal is often to find appropriate Hildebrand and HSP measurements for the nanoparticles. For example, the dispersability of single-walled carbon nanotubes have been measured in large amounts of solvent with varying Hildebrand and HSP [94]. In another study, the Hildebrand solubility parameter for boron nitride nanotubes was studied using light-scattering experiments [95].

In Paper IV, both Hildebrand and HSP were used to develop a rough and simple method to predict the dispersability of CNC in a hydrophobic polymer (in this case LDPE). The CNC was surface-modified with substituents with different carbon chain lengths attached.

MASS TRANSPORT IN POLYMER FILMS

Barrier properties can be evaluated by measuring permeability. While many studies have focused on measuring gas and water vapor permeability, we have used a highly sensitive method to measure diffusion of permeants dissolved in water through film materials. This section is aimed to give a short introduction to permeability and explain the experimental set-up used in this thesis work. Theories aimed to explain permeability results for composites and laminates are also discussed.

4.1. Introduction to Mass Transport

Polymers are often permeable to small molecules like gases, water vapor, and low molecular-weight compounds. According to Henry's law for gases, the permeability of a low molecular-weight chemical compound in a polymeric film depends on the solubility and diffusivity of the permeant [3, 4]. In a first step, the permeant is dissolved into the film surface facing the higher concentration. This is followed by molecular diffusion of the permeant into the film before the permeant dissolves from the film surface again, as shown schematically in Figure 4.1. This process is described in the solution-diffusion model, introduced in 1866 by Graham [99]. The solubility (or partition) coefficient is thermodynamic in nature, and is defined as the ratio of the equilibrium concentration of the dissolved permeant in the polymer to its concentration in the external phase. The diffusion coefficient is the average ability of the permeant to move through the polymer, and it can be determined from Fick's first law as discussed in section 4.1.1.

Factors known to affect the barrier properties and hence the permeability of a polymer are crystallinity, the addition of fillers (especially if they are totally impermeable), the addition of compatibilizers and/or plasticizers, and the chemical structure of the polymer (molecular weight, cross-linking, tacticity) [3, 4, 6]. In general, two types of models explain permeability and mass transport mechanisms in a polymer. The first ones cover molecular models, which focus on the motion of the polymer chains and the permeant in combination with intermolecular forces. The second ones are models of free volume that consider the relationship between the diffusion coefficient and the free volume present in the polymer [5]. Extensive reviews of these models can be found elsewhere [100, 101].

Mass transport properties also depend on whether the polymer is in the rubbery or glassy state [5]. Rubbery polymers are above their glass transition temperature and react quickly to physical changes. This means that a permeant can plasticize a rubbery polymer, which results in increased permeability. Glassy polymers are below their glass transition temperature and do not respond as quickly to physical changes. Mass transport is then believed to occur under non-thermodynamic equilibrium conditions. For these cases a *dual-mode sorption* model can describe the transport mechanism following the model of Henry's law and the transport of the permeant through fixed microcavities present in the polymer.

The size and shape of the permeant also affect its transport through the polymer. For example, longer permeant chains have been shown to have lower solubility than shorter chains in cross-linked polystyrene [102]. The shape of the permeant is important, and flat chains or elongated molecules have higher diffusion coefficients than spherical molecules of equal molecular volume [103, 104]. This has been explained by the orientation of the anisometric molecules along their long axis [103]. At the same time, a larger molecule is more prominent in plasticizing the polymeric barrier than a smaller molecule [105]. Plastization of the barrier in turn increases both the diffusivity and solubility of a permeant and contributes to increased permeability of the barrier.

4.1.1. Measurements of Mass Transport in Films

The primary mechanism [4] for mass transport of a permeant through a defect-free barrier film is diffusion, driven by the concentration gradient created in the experimental setup. Molecular diffusion in one dimension can be described by Fick's first law:

$$J = -Aj = -D \frac{dc}{dx} \quad (11)$$

where J is the flux, j is the flux per unit area, A is the area exposed to the permeant, D is the diffusion coefficient of the permeant specie, and dc/dx is the concentration gradient in the film. The diffusion coefficient is assumed to be independent of position and time. Furthermore, assuming that a pseudo steady state has been reached, i.e. when the concentration within the film does not vary with time, Equation 11 can be developed into Equation 12:

$$J = \frac{DA}{h} (c_1 - c_2) \quad (12)$$

Mass Transport in Polymer Films

where h is the total film thickness and c_1 and c_2 are the concentrations at the surfaces of the films. When the permeant dissolves in an aqueous solution surrounding the film barrier, Equation 12 presumes that the aqueous boundary layers on both sides of the film do not significantly affect the total transport process. Therefore, c_1 and c_2 can be related to the concentrations in the chambers by incorporating the solubility (or partition) coefficient, K (i.e., the ratio between the concentration in the chamber and the surface of the film; see Figure 4.1 for abbreviations):

$$K = \frac{c_1}{c_d} = \frac{c_2}{c_a} \quad (13)$$

where c_d and c_a are the concentrations in the donor and acceptor chambers, respectively, which are possible to measure experimentally.

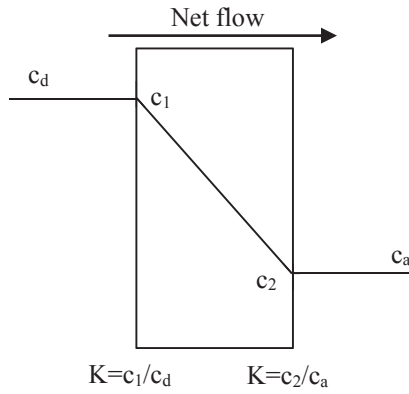


Figure 4.1. Schematic image of the transport through a film at steady state where the partition coefficient $K=1$.

When the concentration of a permeant is the same at the surface of the film as in the concentration chamber, the partition coefficient is $K=1$ (see Figure 4.1). Furthermore, Equations 12 and 13 can be rewritten into Equation 14:

$$J = DKA \frac{(c_d - c_a)}{h} = PA \frac{(c_d - c_a)}{h} \quad (14)$$

The diffusion coefficient (D) times the solubility coefficient (K) gives the permeability (P) for a permeant according to Equation 14. The solubility coefficient should be independent of the concentration if a linear relationship is to be achieved. Diffusion only takes place in one direction for a Fickian behavior to be valid.

However, it has been pointed out that when steady state is slow to be reached or when D and K are correlated to an interaction between permeate and polymer film, Fickian behavior will be replaced by non-Fickian behavior [106].

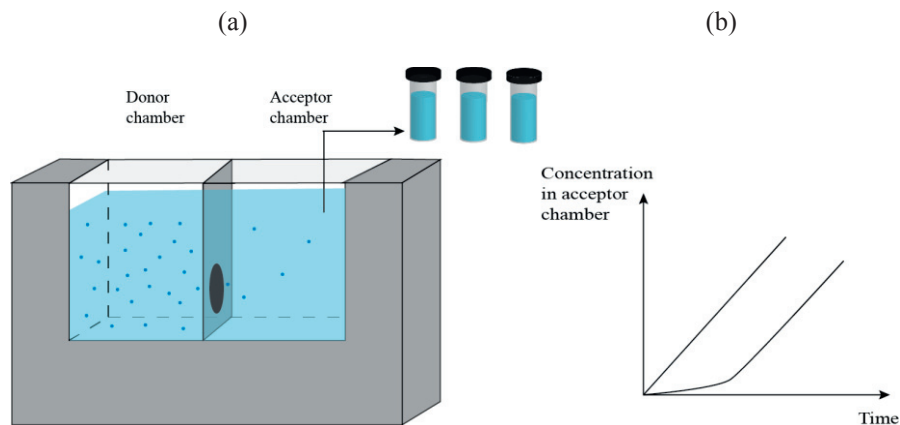


Figure 4.2. (a) Schematic image of a diffusion cell used in the measurement for permeability. A labelled radioactive molecule was added to the donor chamber and samples were collected from the acceptor chamber over time. (b) Suggestions of the results received from a permeability measurement where the accumulated concentration in acceptor chamber is plotted against time.

The experimental set-up used for mass transport studies in all papers is presented in Figure 4.2a. The diffusion cell consists of a donor and acceptor chamber where a film with known thickness is placed between the two chambers. A radioactive molecule is added to the donor chamber and samples are taken from the acceptor chamber over hours, weeks, or even months depending on the material and the permeant. The accumulation of permeant in the acceptor chamber is measured using a liquid scintillation counter and plotted against time as shown in Figure 4.2b. The linear part of the graph is used to calculate permeability according to Equation 14.

4.2. Mass Transport in Composites

The permeability of small molecules through a polymer is determined by their solubility and diffusivity according to Equation 14. Moreover, the addition of a filler in a polymer matrix affects total permeability. This effect will be largest close to the filler, more precisely in the interface formed between the matrix and the filler and at least one polymer radius of gyration (R_g) away from the filler surface [77]. A filler, especially an impermeable filler, will decrease the composite's solubility to less than that of the pure polymer. Transport through the film is affected by the shape and aspect ratio of the filler, but several other factors, including dispersion, adhesion to the matrix, filler-induced solvent retention, and porosity, are also important [40, 77, 107, 108]. Incorporating a totally impermeable filler can increase the tortuosity path for a permeant [6], resulting in a longer path through the material, leading to a slower diffusion process and hence a lower permeability. Figure 4.3a shows the average tortuosity path through a polymer matrix without any added filler, while in Figure 4.3b, the added fillers are perfectly aligned. Figure 4.3c, in which the fillers are randomly placed, shows another example of the increased tortuosity caused by the presence of fillers.

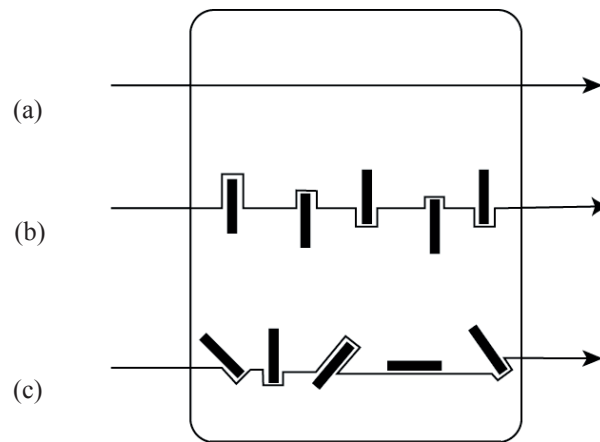


Figure 4.3. Schematic image of how fillers can affect the transport path through a composite (a) pure matrix, (b) perfectly aligned fillers, and (c) randomly aligned fillers.

Theoretical approaches often treat fillers as impermeable non-overlapping particles and assume no permeability changes in the polymer matrix [6, 7]. The permeability

of such systems, in which the fillers are completely aligned or randomly distributed, was first calculated by Nielsen in 1967. The basic idea is that the filler contributes an increased tortuosity path for the permeant; the permeability for the composite was derived to (Equation 15):

$$\frac{P_{comp}}{P_{poly}} = \frac{1-\Phi}{1+a\Phi} \quad (15)$$

where a is the filler aspect ratio (for square fillers) and Φ is the volume fraction of the filler [6]. This model has been shown to correlate well to a material of maximum 5 wt% CNC and PLA, where the permeability of water and oxygen have been reduced [35]. In 2001, this model was further developed to account for non-aligned fillers by introducing an order parameter S for the filler orientation [7]:

$$\frac{P_{comp}}{P_{poly}} = \frac{1-\Phi}{1+a\Phi^2(S+\frac{1}{2})} \quad (16)$$

Equation 16 reduces to Nielsen theory for perfectly aligned fillers if $S=1$. The conclusions from the theories are that it is possible to receive similar permeability for perfectly aligned fillers compared with randomly aligned fillers with similar aspect ratios [77]. However, higher amounts of the randomly aligned filler is needed to obtain comparable results. The importance of the filler orientation decreases with increasing aspect ratios. Nielsen has also derived equations for cases when channels are formed between the filler and the matrix, or when the filler does not disperse and instead forms porous aggregates [6].

Fillers may also function as nucleating agents and induce crystallinity in the matrix polymer [31-34]. Filler-induced crystallinity is thought to increase the tortuosity in the composite due to its low permeability, leading to slower diffusion processes and reduced permeability of the composite [77, 109, 110]. In this thesis, cellulose was used as filler, and it should be taken into account that cellulose is not totally impermeable to water. CNCs have been shown to have lower permeability than cellulosic fibers [36], and recent studies have shown that the addition of cylindrical cellulose nano-rods can result in pore formation in the matrix material [9, 12, 16, 35, 37, 39, 111]. The presence of pores is expected to increase permeability and the number of pores seems to increase with increased added filler. One study showed that the addition of 1 wt% CNC was enough to result in a material with 9% porous material compared with the pure matrix that was only 1% porous [37]. Another way to acquire increased permeability is to make the interface more favorable for diffusion either by poor adhesion between the filler and the matrix or as shown in Paper I [76], where the surface of cellulose was modified with a hydrophilic polymer. Both scenarios are expected to result in increased permeability.

4.3. Mass Transport in Laminates

As previously discussed, permeability depends on solubility and diffusivity, according to Equation 14. Solubility can be described by the partition coefficient, K , for a single-layered film. If the partition coefficient is equal to 1, the concentration of permeant is the same in the interior of the film surface as at the surface of the outside of the film (see Figure 4.1). This results in a linear concentration decline within the film, going from the concentration in the donor chamber, c_d , to the concentration in the acceptor chamber, c_a . This is not often the case for solid films, and Figure 4.4a shows a case with the partition coefficient $K \ll 1$, meaning that the concentration is higher on the surface of the film than in the interior. Figure 4.4b shows the same scenario as for the single-layered film, but for a laminated film. In this case, there is no contribution from the interface to total mass transport over the film. This also means that the partition coefficient for the interface needs to be equal to $K_{AB} = 1/K_{BA} = K_B/K_A$.

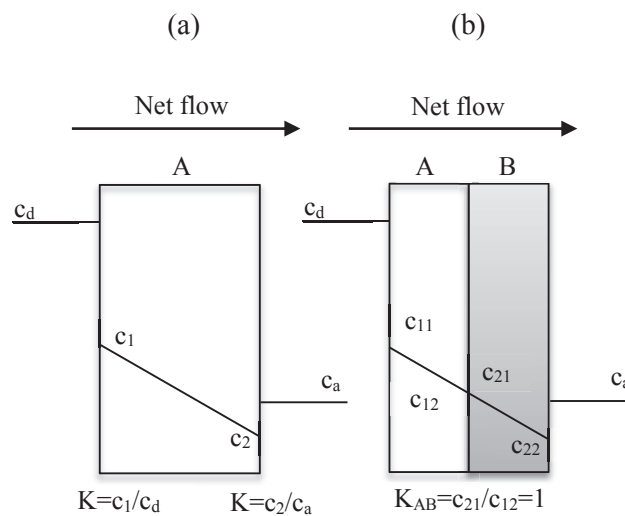


Figure 4.4. Schematic images of the mass transport through (a) a pure film where $K \ll 1$ and (b) a two-layered film where $K_{AB} = 1$ resulting in linear concentration declines in the films.

Permeability of laminates with defect-free polymeric layers can be described by the Ideal Laminate Theory, given by Equation 17 [112]:

Mass Transport in Polymer Films

$$\frac{h_{\text{tot}}}{P_{\text{tot}}} = \sum_1^n \frac{h_i}{P_i} \quad (17)$$

where P_i and h_i are the permeability and the thickness of each layer, respectively. This equation assumes that the mass transport, dm/dt , is the same regardless of the order of the individual layers [112, 113], as shown in Figure 4.4.b. For a film A with the solubility coefficient K_A and a film B with solubility coefficient K_B , this equation is valid only in the case when $K_{AB}=1/K_{BA}=K_A/K_B$, meaning that there is no difference of permeability regardless of how many layers in the film. The equation also assumes that there is no contribution of the interface to the total mass transport over the material. It is, however, possible to add an extra term to Equation 17 [114] to include the effect of the interfaces in the total transport:

$$\frac{h_{\text{tot}}}{P_{\text{tot}}} = \sum_1^n \frac{h_i}{P_i} + \sum_1^n \frac{h_{\text{int}}}{P_{\text{int}}} \quad (18)$$

where h_{int} and P_{int} are the thickness and permeability of the interfaces in the film. This additional sum includes all the interfaces present in a layered film, but the condition of $K_{AB}=1/K_{BA}=K_B/K_A$ must still be valid.

EXPERIMENTAL OVERVIEW

This chapter provides an overview of the experimental work, illustrated in Figure 5.1. More details can be found in the papers themselves. Basically, the work was divided into two parts covering (i) composites and (ii) laminates. The part dealing with composites was further divided into two cases: the first examined surface modification of the filler by adsorption, resulting in Paper I; the second examined chemical surface modification and resulted in Paper II-IV. Paper V discusses the work with laminates. The experimental set-up was similar in all papers, with the focus on measuring mass transport properties as described in Chapter 4.

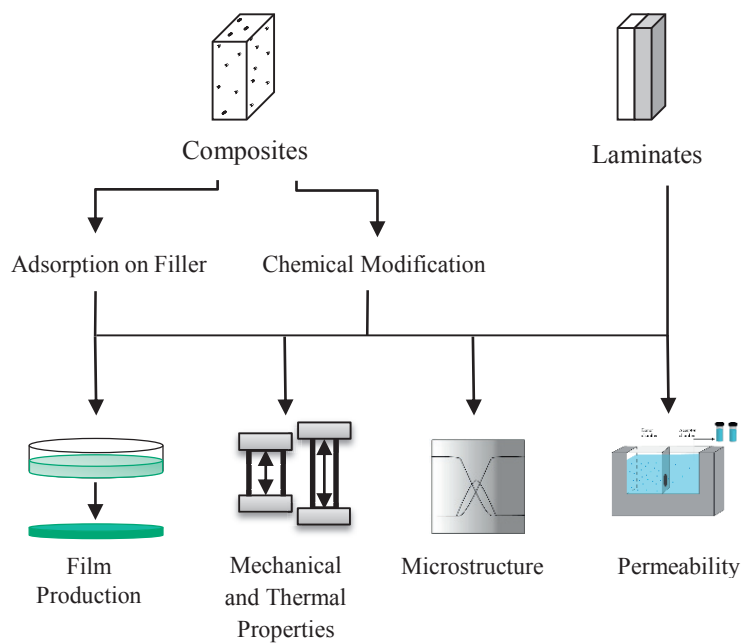


Figure 5.1. Overview of the experimental part of the project.

Film production has been important throughout the project, and several methods such as solvent casting, spin-coating, extrusion, and hot-melt pressing were used. The major challenge was to produce homogenous film materials, especially in the case of nanocomposite films, where the CNC was difficult or impossible to disperse in most

Experimental Overview

organic solvents. In these cases, solvent casting had to be combined with hot-melt pressing to disperse the nano-fillers more homogeneously. For the composite films with added microcrystalline cellulose (MCC), extrusion was followed by hot-melt pressing. All composite films were produced in lab-scale, while the laminates were produced via extrusion at Tetra Pak, Lund.

To increase the compatibility of cellulose in the more hydrophobic polymers, the surface was modified in different ways. In the first case, simple adsorption to the surface of MCC was performed in a water suspension overnight, followed by freeze-drying. For the chemical surface modification of CNC, different chemical reaction conditions had to be tested and evaluated. One reaction used was a ring-opening polymerization of lactic acid, where we explored the surface coverage as well as the lengths of the attached chains. Surface modification of cellulose was characterized using techniques such as Fourier-Transform Infrared Spectroscopy (FT-IR), which is a quick and easy method to obtain information about chemical composition. However, this technique is not quantitative and does not provide any information about the lengths of the attached chains or the surface coverage. Solid-state NMR can be used for quantitative analysis, and Paper II discusses our extensive study of the surface modification of CNC by this method. Elemental analysis, which is a much quicker method compared to solid-state NMR, was also used to confirm successful surface modification. This method can be used to determine the amount of various elements in a chemical compound. We used this method when the chlorohydrins were attached to the surface of CNC, since there are nitrogen present in the substituents but not in the lactic acid, which consists only of carbon, oxygen, and hydrogen, similar to CNC.

Thermal properties and crystallinity were studied using differential scanning calorimetry (DSC). DSC is used to study phase transitions (e.g. melting when energy is needed or crystallization when energy is liberated) for polymers. A sample is placed in a beaker next to an empty reference beaker. The amount of added or liberated energy is then recorded as temperature increases or decreases. It was important to measure the crystallinity of the produced films to understand and explain the results for mass transport, since the crystalline parts of a materials are considered impermeable.

Mechanical and/or viscoelastic properties were measured for the composite films in Papers I, II, and IV. Viscoelastic properties were measured using dynamic mechanical analysis (DMA), in which sinusoidal stress is applied to a film material. At the same time, relative humidity was varied. This was done to study the adhesion between MCC and PLA, as well as between surface-modified MCC and PLA as relative humidity increased from 10% to 90%. DMA can also be used to measure

Experimental Overview

creep-recovery properties when applying a constant force to the film material. This was used to compare adhesion between unmodified and modified CNC in a matrix of LDPE.

Microstructure was evaluated using techniques such as visual inspection, polarized microscopy, and scanning electron microscopy (SEM), with SEM having the highest resolution. Polarized microscopy has a theoretical resolution down to approximately 200 nm, and the method was used when large aggregates were formed in the nanocomposites. To reveal the interior of the produced films, however, SEM was necessary. We used SEM mainly to study cross-sections of the composite films, which were fractured by being in liquid nitrogen and cracked with a pair of tweezers. Because the polymer films were non-conducting, we coated the surface with a thin film of gold prior to SEM analysis.

A comprehensive study was performed on the interfaces between two polymers, and the chemical composition of the interfacial layer was evaluated using time-of-flight secondary ion spectrometry (TOF-SIMS). TOF-SIMS has a resolution in the nanometer range and in this case depth-profiling was performed to reveal the composition of the interface between the two polymers in the laminates. Crystallinity and ordering close to the interface was also studied using SAXS and WAXD.

OUTCOME OF RESEARCH

This chapter summarizes the main finding in this project; further details can be found in each paper. The impact on mass transport is discussed in relation to composites in part 6.1 and to laminates in part 6.2.

6.1. Mass Transport of Water in Composites

6.1.1. *Surface-Modified Cellulose via Adsorption*

To test whether it is possible to create a composite material with increased mechanical properties and the same time control for water permeability, the microscale cellulose filler MCC was added to a matrix of PLA (Paper I). The surface of the filler was modified by simple adsorption of a hydrophilic polymer prior to film production, which resulted in various interfaces. The hydrophilic polymer was in this case xyloglucan, which is a hemicellulose present in pulp and elsewhere. Cellulose and xyloglucan were mixed in a water suspension overnight. The water suspensions were freeze-dried and films produced via extrusion followed by hot-melt pressing. The films consisted of ~20% cellulose and 80% PLA, while the addition of xyloglucan (XG) varied between 4 and 50 mg/g cellulose. The highest amounts were expected to totally coat the surface of the microcrystalline cellulose [115, 116]. As a comparison, two materials consisting of either pure PLA or a composite of cellulose and xyloglucan were produced without the pre-adsorption step. Our hypothesis was that we could increase adhesion between the filler and the matrix in a composite by adsorbing xyloglucan on the surface of cellulose. This hypothesis was based on previous findings by Raj and co-workers, who used atomic force microscopy (AFM) to measure the adhesion force between PLA-cellulose and PLA-xyloglucan and showed an increased adhesion of PLA to xyloglucan compared to cellulose [15].

To study the adhesion between the matrix and the filler, viscoelastic properties were measured for the films as the relative humidity was increased from 10% to 90% over 16 hours. Figure 6.1a shows the storage modulus against the relative humidity. Storage modulus was lowest for the pure PLA film, closely followed by the composites with microcrystalline cellulose. The addition of xyloglucan resulted in increased storage modulus and in general, the more added xyloglucan, the higher the storage modulus. These results indicate a better adhesion between the matrix and the filler, and hence a stronger composite, at lower relative humidity. However, at a

relative humidity higher than 50%, the storage modulus was affected by the addition of xyloglucan and an increasing slope can be seen between a relative humidity ranging from 50% to 90% (green arrow in Figure 6.1a shows the slope for the pure PLA film as an example). The slopes in this interval are shown in Figure 6.1b, where pure PLA has the lowest slope and the cellulose particles covered with the highest amount of xyloglucan has the highest slopes. For the cellulose particles with no xyloglucan adsorbed to the surface in the pre-step, the impact of relative humidity is smaller. The explanation is most likely increased capillary forces created between the pre-adsorbed filler and PLA, hence an increased adhesion when a more hydrophilic polymer is adsorbed on the surface [15, 76, 117].

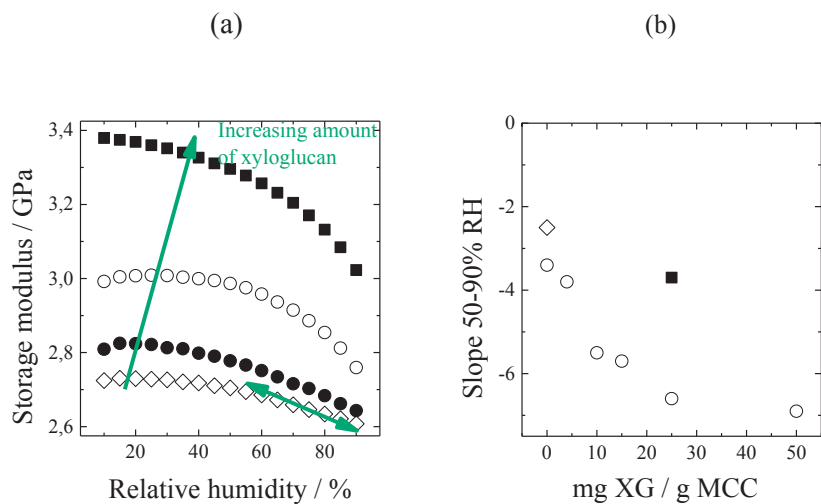


Figure 6.1. Storage modulus as a function of relative humidity for (a) PLA (\diamond) PLA-MCC (\bullet), PLA-XG films (\circ), and (\blacksquare) and (b) the slope of the storage modulus in the humidity range of 50-90% RH for the pure PLA film (\diamond) and the composites (\circ). The storage modulus for the film without the pre-adsorption step is also shown (\blacksquare).

Figure 6.2 suggests an explanation for the reduced storage modulus at higher relative humidity, which is believed to be due to reduced capillary forces between the filler with adsorbed xyloglucan on the surface and the matrix. The size of the arrows are meant to visualize the capillary forces, with forces larger at lower relative humidity and smaller at higher relative humidity. For the unmodified fillers, the storage modulus was similar to PLA, hence no xyloglucan is present to induce capillary

forces. These reduced capillary forces have also been observed and discussed in other studies. For example, Raj and co-workers measured the adhesion between PLA and cellulose by AFM and showed that the adhesion force was dominated by capillary forces up to ~70% RH [15]. Xiao and co-workers also measured the adhesion force between a hydrophilic SiO₂ surface and a hydrophobic AFM tip of Si₃N₄ [117]. At a relative humidity above 80% the adhesion force decreased drastically, also explained by reduced capillary forces at a higher relative humidity.

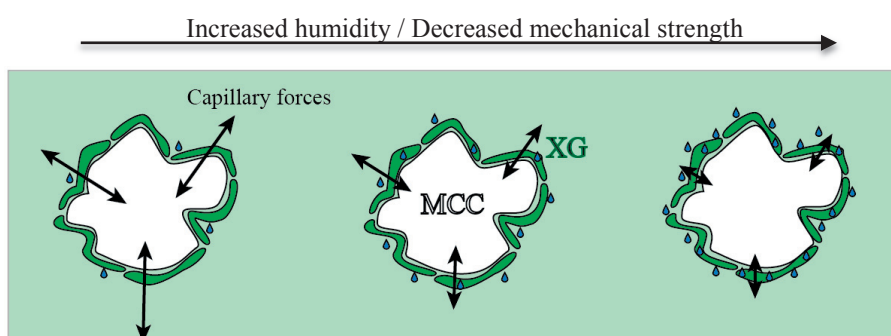


Figure 6.2. Schematic images of the decreased capillary forces at higher relative humidity, resulting in a decreased storage modulus. Note the small water droplets which symbolize the presence of water in the material.

In a water permeability experiment, the films are exposed to 100% relative humidity, meaning that the addition of the hydrophilic xyloglucan should affect mass transport. The accumulation of labelled water is plotted as a function of time in Figure 6.3a, where the pure PLA film is compared with a film with 50 mg xyloglucan/g cellulose. The film with 50 mg xyloglucan shows a much faster accumulation of labelled water in the acceptor chamber compared to the pure PLA film. Figure 6.3b shows the calculated water permeability for all films. The lowest water permeability is observed for the pure PLA film, while the addition of MCC increased the water permeability by a factor of two. The increased water permeability may be a result of the poor adhesion between PLA and cellulose. The adsorption of increasing xyloglucan onto the surface resulted in increased water permeability, however, the water permeability is similar for the materials with 25 and 50 mg XG/g MCC. The maximum value of adsorption has been previously reported [115, 116]. Considering that hemicellulose is more hydrophilic, increased water permeability with higher additions is not surprising, but opens the possibility in material design for materials with water permeability that can be controlled for various final applications.

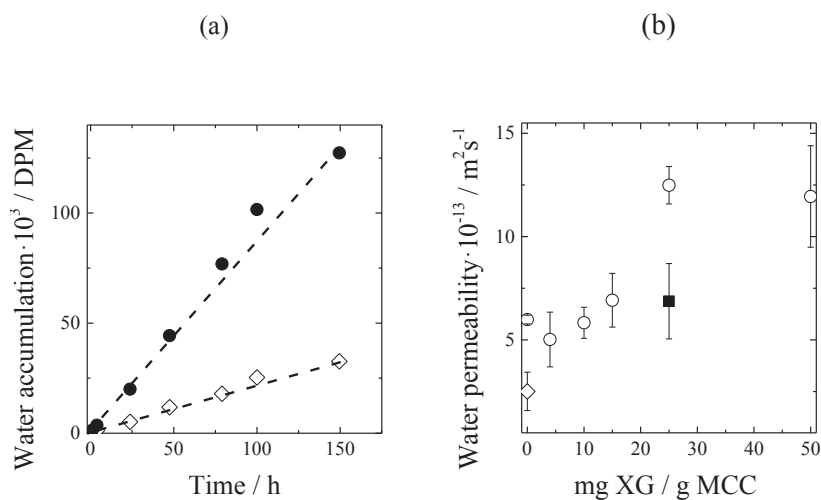


Figure 6.3. Data from permeability measurements showing (a) water accumulation as a function of time in the acceptor chamber for the pure PLA film (\diamond) and a composite film with 50 mg XG/g MCC (\bullet) and (b) water permeability of PLA and pre-absorbed XG:MCC particles with increasing amount of XG per gram MCC (\circ), pure PLA (\diamond) and composites of PLA:XG:MCC (\blacksquare), where no pre-absorption step was done.

Figure 6.4 shows water permeability as a function of crystallinity for the composites. The pure PLA film showed a crystallinity of 1% and also the lowest water permeability. Adding the filler resulted in increased crystallinity. It is interesting that even though we had increased crystallinity with the addition of MCC and MCC-XG, we still observed increased water permeability. This means that it is possible to produce materials with higher crystallinity, increased mechanical properties, and increased permeability. However, it seems to be important to have control over where the xyloglucan is located in the composite. It seems likely that composites with the xyloglucan adsorbed to the surface follow a more or less constant increase in permeability, while the films with the xyloglucan simply mixed in does not follow the same trend.

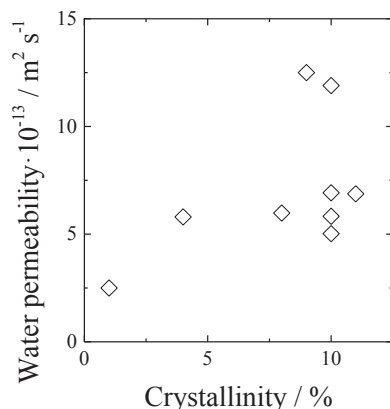


Figure 6.4. Water permeability as a function of crystallinity, in which PLA shows the lowest crystallinity and water permeability.

In summary, Paper I showed that water permeability can be influenced if a hydrophilic polymer is added to a composite. It is, however, important to have control over the location of the hydrophilic polymer; the increased water permeability and increased storage modulus were only observed when the hydrophilic polymer was pre-adsorbed to the surface of the microcrystalline cellulose particles.

6.1.2. Chemical Surface Modification of Cellulose

Good compatibility between the matrix and the filler of a nanocomposite is important for the dispersability of the filler but also for the production of homogenous nanocomposites. CNCs have been widely studied due to their defined morphology and reinforcement properties for different polymers [24, 36]. The nano-fillers are often produced via acid hydrolysis, where the amorphous parts are cut off as shown schematically in Figure 6.5. To increase compatibility between CNC and two biodegradable polymers, PLA and PLGA, the surface of the filler was modified with PLA chains as shown in Figure 3.4 [80, 108]. So far, few studies have focused on quantitative calculations of the surface coverage of the substituent, which we attempted in Paper II. Additionally, recent studies have shown that the addition of a surface-modified nano-filler can result in a porous film material [12, 35, 37, 39]. However, the mechanism for this formation has so far not been discussed in literature.

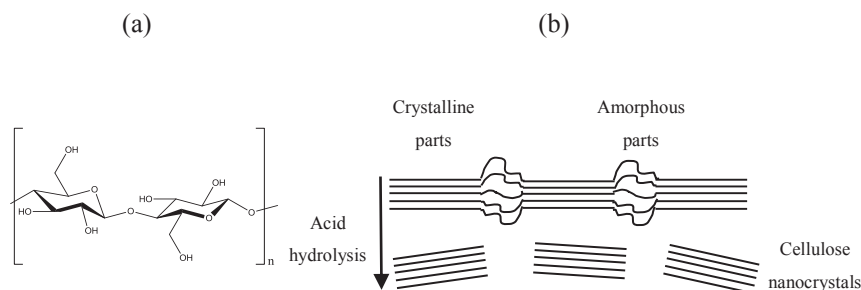


Figure 6.5. (a) Chemical structure of cellulose, (b) schematic image of production of cellulose nanocrystals via acid hydrolysis.

The successful modification was confirmed using solid-state NMR. A quantitative analysis also showed that approximately half of all available reactive groups on the cellulose surface had PLA chains attached. Furthermore, it was shown that on average only one ring (or two lactic units) had been attached to the surface, meaning that only short substituents were sticking out from the surface. However, these short chains were still enough to get different colloidal behavior in various solvents (see Figure 3 in Paper II), where unmodified CNC dispersed well in water but formed large aggregates in the more nonpolar dichloromethane. For the modified CNC, sedimentation was observed in water, while it dispersed well in dichloromethane. Dichloromethane was the solvent we used for film production, hence it was important that the CNC dispersed well in that solvent to avoid aggregate formation in the final nanocomposite films.

Nanocomposites, with both PLA and PLGA used as matrices, were produced by solvent casting, and water permeability was measured, as presented in Figure 6.6a-b. The expected permeability according to Nielsen theory (Equation 16) for perfectly aligned (dashed line) and random fillers (straight line) is also shown in all graphs. Figure 6.6a shows the results for PLA nanocomposites, with the pure PLA film showing the lowest water permeability. The addition of both unmodified and modified CNC resulted in higher water permeability. The experimental results are also well above the calculated values of the theoretical permeability for both aligned and random filler. For PLGA nanocomposites, the experimental data are closer to the theories, except for the 20 wt% film that is well above the theoretical projections (Figure 6.6b).

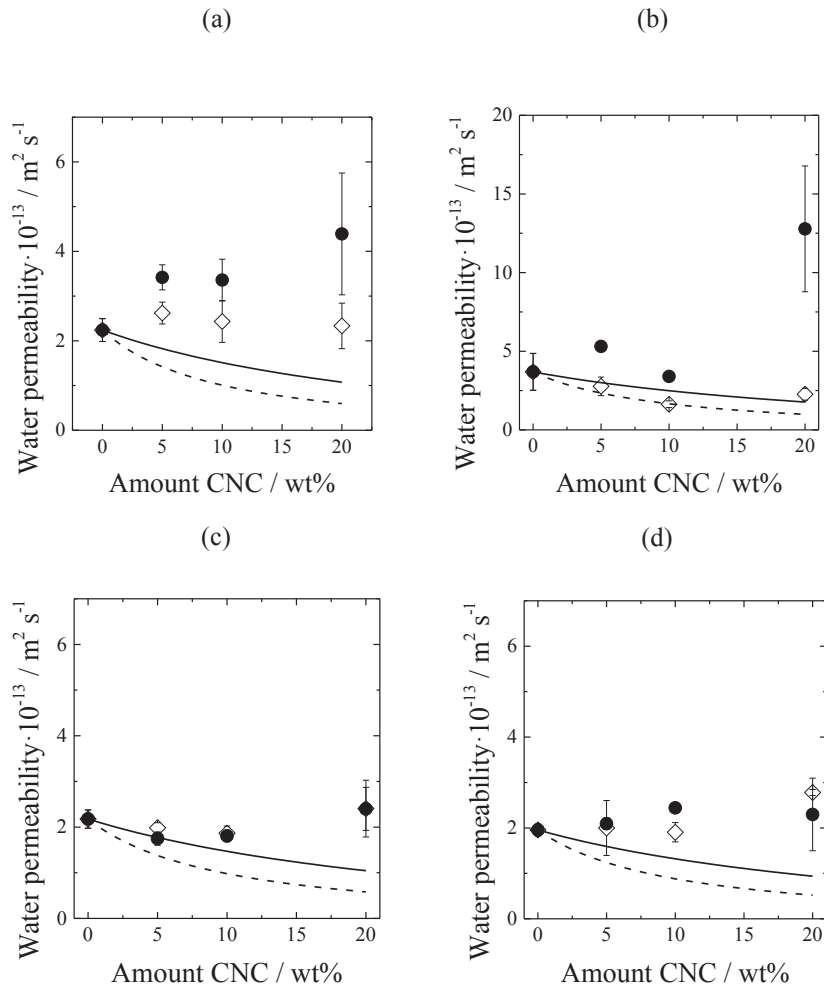


Figure 6.6. Water permeability for solvent casted films (a) PLA, (b) PLGA, and the hot-melt pressed films (c) PLA and (d) PLGA, with CNC (\diamond) and mod-CNC (\bullet) composites. Note that the scales are different in the graphs. The theoretical values using Nielsen model (Equation 16) with perfectly aligned cylindrical nano-fillers is plotted as a dashed line and the straight line shows random distribution.

In recent years, several studies have shown pore formation in matrix material after the addition of a rod-like filler [12, 35, 37, 39, 111]. From results and observations in previous studies we suspected that we had pore formation in the nanocomposites with the addition of the modified CNC. Therefore, we decided to hot-melt press the

Outcome of Research

films and repeat the water permeability experiment, as shown in Figure 6.6c-d. Water permeability in these films was more or less constant, and also closer to the Nielsen theory for randomly aligned fillers. Therefore, there is reason to believe that we reduced the number of pores, but since the theories are not appropriate with measured values, there are probably also remaining pores in the films after hot-melt pressing. To discover whether pores were present, we measured the density of the different films (see Figure 3 in Paper III for results). The results showed that pure films had values close to expected (PLA=1.25 g/cm³ and PLGA=1.30 g/cm³, respectively) both for solvent casted and hot-melt pressed films. Adding CNC to PLA or PLGA was expected to result in increased density since CNC has a density of 1.6 g/cm³ [118]. Instead, the addition of unmodified CNC had no effect on the density for the solvent casted films, while the density decreased when modified CNC was added, in both PLA and PLGA nanocomposites. In general, the higher the amount of added modified CNC, the more the density decreased. However, after hot-melt pressing the density of all films was more or less constant. Therefore we believed that some pores remained in the nanocomposites even after hot-melt pressing, which is one explanation for the observed permeability. Another possible explanation is that cellulose is not perfectly impermeable to water, and hence the expected permeability is not observed upon addition of these nano-fillers.

The cross-sections of the nanocomposite films of both PLA or PLGA and CNC are shown in Figure 6.7. In order to reveal the interior, films were placed in liquid nitrogen for 5 to 10 minutes and then carefully broken into two pieces with two pairs of tweezers. SEM studies of the interior of the nanocomposites showed pore formation in the films where the mod-CNC had been added. The pure films have a smooth interior, while the addition of both unmodified and modified CNC created some irregularity in the cross-sections. In films with modified CNC this is seen as pores in the micrometer scale for both PLA and PLGA (shown with green arrows).

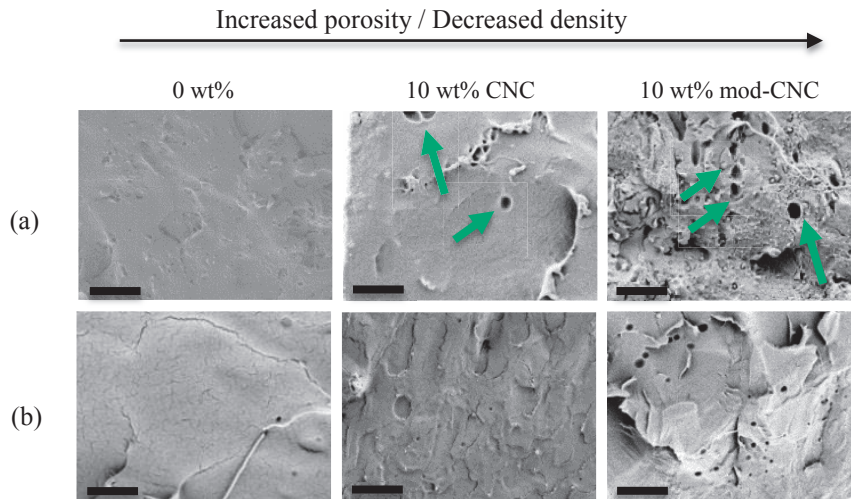


Figure 6.7. SEM images of the cross-sections of (a) PLA and (b) PLGA and the respective composites (SE detector, 10kX magnification). Scale bar is 5 μm and arrows show pores.

Figure 6.8 shows water permeability as a function of crystallinity for the nanocomposites of PLA (PLGA was totally amorphous and is therefore not shown). As in the study with PLA, cellulose, and xyloglucan, it is possible to see increasing water permeability upon higher crystallinity: the opposite of what is expected. However, in this case pore formation explains the higher water permeability.

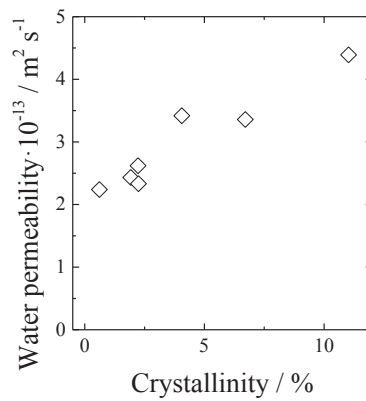


Figure 6.8. Water permeability as a function of crystallinity for the PLA composites with cellulose nanocrystals.

Outcome of Research

In Paper III, we suggest a probable mechanism for pore formation upon the addition of rod-like nano-fillers to a polymeric matrix when the fillers are well dispersed in the solvent/matrix. Briefly, the pore formation can be explained by the formation of a locked network of the cylindrical nano-filler [119]. When solvent casting is used as a production method, the polymer is dissolved in a suitable solvent, which results in increased viscosity. Adding nanoparticles to this suspension will result in an even higher viscosity. It has been shown that the addition of 3.5 wt% CNC produced via sulfuric acid hydrolysis to water increases the viscosity 10^6 times compared with pure water at low shear rates, explained by the formation of liquid crystalline phases [120]. Furthermore, the viscosity depends on the volume fraction, particle size, attractive van der Waals interactions between the fillers, and possible aggregation of the filler [119, 121-123]. The overlap concentration for the nano-fillers depends on the aspect ratio, and is often very low for a filler in the nanoscale (often a few percent) [119]. This means that at a certain point during the solvent evaporation (and film production) the rod-like nano-fillers will start to permanently overlap, which results in a locked network if the nano-fillers are well dispersed. In the case of aggregate formation, as for the unmodified CNC, the same increase in viscosity is not expected, and the final film will be inhomogeneous with aggregates present. Figure 6.9a shows a schematic image of the vials prior to solvent casting. In the case of unmodified CNC there is aggregate formation already in the polymer solution, these aggregates are also present in the final nanocomposite. The surface-modified CNCs are well dispersed in the polymer solution, but as the solvent evaporates the rod-like nano-fillers form a locked network and the polymer cannot precipitate along the modified CNC in the locked system, which results in pore formation. Figure 6.9b shows a schematic image of the film prior and after hot-melt pressing, in which the same mechanism as in solvent casting is believed to occur, even though we successfully reduced the amount of pores for these films. The reduction of pores is believed to be due to the pressure deforming the overlapped and percolated network of the nano-fillers, making it possible for the polymers to precipitate along the nano-fillers.

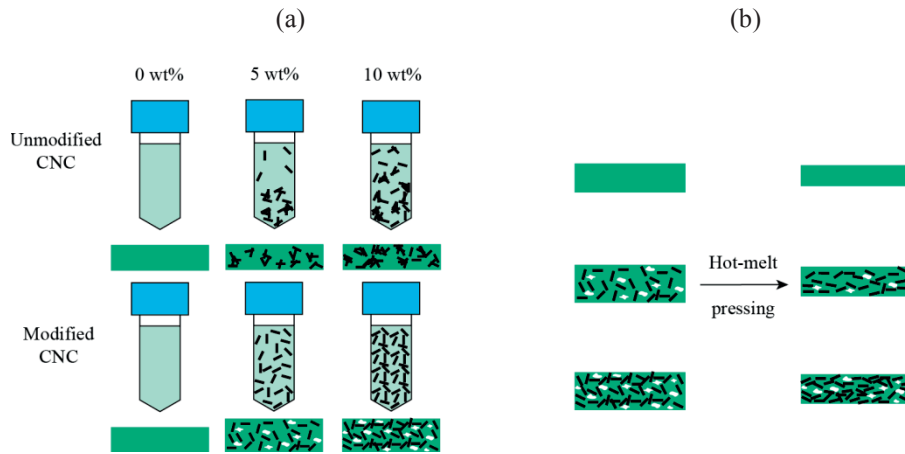


Figure 6.9. Schematic images of (a) the solvent evaporation and film formation where unmodified CNC (upper row) and modified CNC (lower row) is dispersed in a polymer solution and (b) films before and after hot-melt pressing. Pores are present in both cases.

In summary, the results in Papers II and III showed that it is possible to create nanocomposites with increased or decreased water permeability. The major challenge when producing these nanocomposites is to obtain a homogenous dispersion of nano-fillers in the matrix. This can be achieved by surface modification of the filler, but a result of well dispersed nano-fillers is pores in the final nanocomposite. These pores are also difficult to remove by hot-melt pressing and should be taken into account when producing nanocomposites with rod-like fillers.

6.1.3. Prediction of Dispersability of Nano-Fillers in Polymers

As we learned in the previous study, it is often difficult to predict the dispersability of modified CNC. Therefore, we wanted to develop a simple and straightforward method using HSP and varying solvents. In this study, we used another modification of CNC, where a Y-shaped molecules (Figure 6.10) were covalently attached to the surface of CNC. This second surface modification was chosen because we could control the chain lengths attached to the surface in a better way than the surface modification used in Papers II and III. The carbon chains had a length of either 6 or an average of 17 carbon atoms and the successful modification was evaluated using FT-IR and elemental analysis. Approximate HSP values for unmodified and modified cellulose were calculated using the software Hansen Solubility Parameters in Practice. Two glucose units were modified with two substituents according to the inset in Figure 6.11. The tabulated values for different solvents and the calculated values of dispersive, polar, and hydrogen parts of the HSP are shown in Figure 6.11. The values should be as similar as possible to have good compatibility between the solvent and the nanoparticles, as discussed in section 3.3. Cellulose shows values closest to water and methanol, while the modified cellulose shows values closer to butanol and dichloromethane.

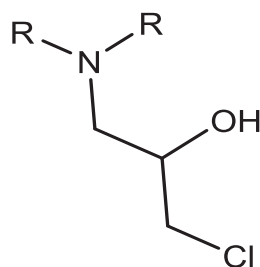


Figure 6.10. Chemical structure of the reactant used in Paper IV. R is equal to either 6 or an average of 17 carbons chains.

The dispersability of both modified and unmodified CNC was tested in the solvents listed in Figure 6.11. As predicted, the unmodified CNC dispersed well in water and methanol (see Figure 4 in Paper IV). It should be noted that the unmodified CNC has sulfate ester groups on the surface that help to stabilize it in water through electrostatic interactions. The modified cellulose with the shorter chains dispersed well in ethanol and butanol which is in accordance with the approximate values presented in Figure 6.11. The modified CNC with longer chains on the surface dispersed well in dichloromethane.

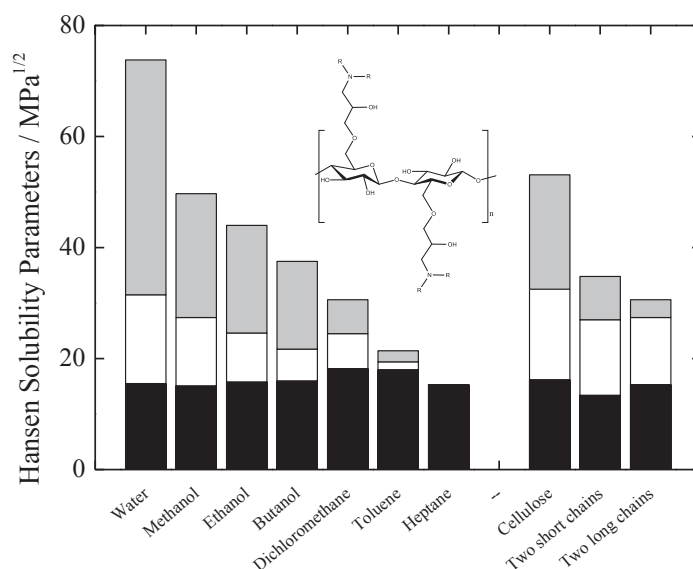


Figure 6.11. Tabulated values of HSP for tested solvents as well as calculated values for cellulose (black parts show the dispersion, white the polar, and grey the hydrogen bonding interactions). Modified cellulose with two chains attached as shown in inset.

It was suggested that the CNC with the longest chains should disperse well in a matrix of LDPE since the HSP are similar for LDPE and dichloromethane. Nanocomposite films of LDPE and both modified and unmodified CNC were produced via solvent casting followed by hot-melt pressing, which resulted in homogeneous films. Creep test of the pure LDPE and the nanocomposite films was performed in a DMA and the results are presented in Figure 6.12a. The nanocomposite with CNC with the longer carbon chains attached to the surface showed the highest resistance to creep, while the addition of unmodified CNC and chains with only 6 carbons did not affect the creeping compared with pure LDPE films. Figure 6.12b shows the recovery of the nanocomposites after 10 minutes of creep. The recovery is quite similar for all materials, however the films with the modified CNC with longer chains did recover slightly faster. These results indicate improved adhesion between matrix and filler when longer chains are attached to the surface of cellulose.

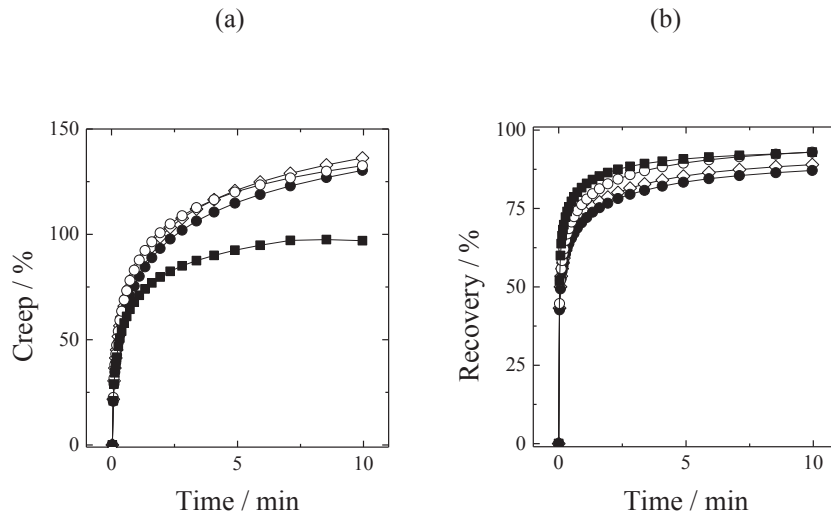


Figure 6.12. (a) Creep test and (b) strain recovery for the LDPE and nanocomposites with 5 wt% CNC added, where LDPE (\diamond), CNC (\bullet), CNC6 (\circ), and CNC17 (\blacksquare) are shown.

Figure 6.13 shows the water permeability of the LDPE nanocomposites as well as the expected permeability according to Nielsen theory for randomly aligned rod-like nano-fillers. The different lines represent different aspect ratios for the nano-filler (straight=10, dotted=50, and dashed=100). The pure LDPE film had a permeability of $6.6 \cdot 10^{-13}$ m²/s while the addition of unmodified CNC resulted in increased permeability compared to the pure LDPE film. This is probably best explained by poor adhesion between the matrix and the filler, but pores may also be an explanation, as discussed earlier. However, the addition of the two modified CNC resulted in a decreased permeability with the longer chains showing the lowest values. According to Nielsen theory, an aspect ratio of 50 to 100 shows the most similar values to experimental data. This is in agreement with values measured using AFM, in which lengths are estimated at 300 to 400 nm and diameters at 5 to 10 nm, resulting in an aspect ratio somewhere between 30 and 80. As discussed in relation to the creep test, this indicates that there is increased adhesion between the matrix and the filler when longer chains are attached to the surface of CNC because water permeability is decreased.

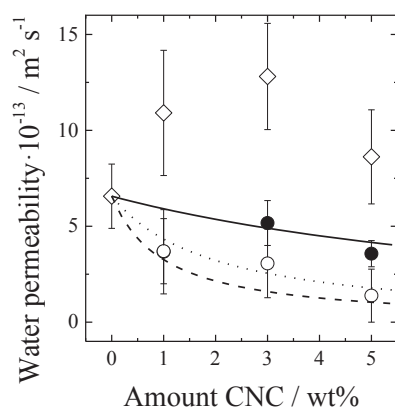


Figure 6.13. Water permeability for LDPE and the nanocomposites with increasing amount of unmodified CNC (◇), CNC6 (●), and CNC17 (○). Lines show calculated permeability according to Nielsen theory for randomly aligned rods; the black line represents an aspect ratio of 10, dotted is 50, and dashed is 100.

In summary, the results from the study suggest that it is possible to predict the dispersability of unmodified and surface-modified CNC fillers in a hydrophobic polymer matrix by the use of HSP. A critical step is the calculation of approximate solubility parameters for the modified fillers, since it can be difficult to know the surface coverage. To simplify this step, only two monomers of cellulose were used as a model; however, the results indicate that the suggested approach is valid. The method developed should only be seen as a first rough step to predict the dispersability in a matrix material.

6.2 Mass Transport of Carboxylic Acids in Laminates

Packaging needs to be strong enough to transport various components of foods. Both oleic and acetic acid are examples of carboxylic acids present in different types of food. Often different combinations of polymers (or other materials) are used in food packaging and hence interfaces are formed between these materials. To investigate whether the presence of these interfaces had any impact on the total mass transport of oleic and acetic acid, the permeability of pure films of LDPE and EAA were measured, as were laminates with 2, 4, or 8 layers. These films were produced via co-extrusion, and the total thickness of each of the films was approximately 100 μm . The permeability of oleic acid and acetic acid, respectively, is shown in Figure 6.14a-b. The grey columns represent the experimental values and the white columns represent calculated (and expected) values according to Ideal Laminate Theory and Equation 17. Figure 6.14a shows the permeability of oleic acid. The highest permeability of $101 \cdot 10^{-15} \text{ m}^2/\text{s}$ was found in the pure LDPE film, while it decreased to $69 \cdot 10^{-15} \text{ m}^2/\text{s}$ for the pure EAA film. Combining the two materials into either 2 or 8 layers resulted in decreased permeability. Similar results were seen for acetic acid, but in this case the permeability was much lower than for oleic acid. In this case, LDPE had a permeability of $2.5 \cdot 10^{-15} \text{ m}^2/\text{s}$ and EAA $2.0 \cdot 10^{-15} \text{ m}^2/\text{s}$. Most interestingly, the expected permeability for the laminates according to Ideal Laminate Theory. These values are indeed much higher than the experimental values. This indicates that the presence of interfaces has a strong impact on the total permeability of a laminate.

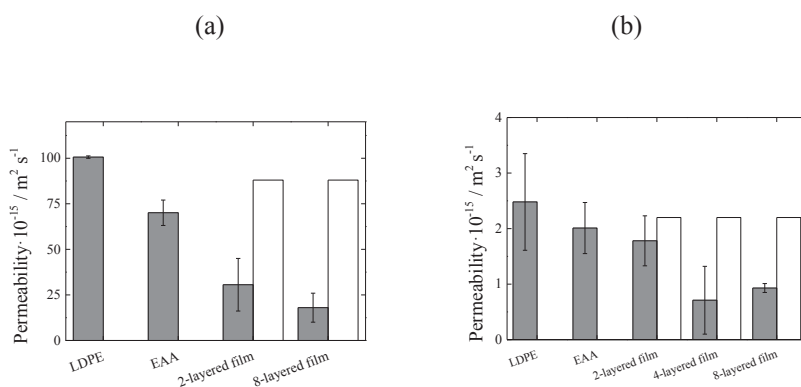


Figure 6.14. Permeability of (a) oleic acid and (b) acetic acid for LDPE and EAA as well as the laminates. Grey columns are experimental data while white columns are calculated values based on Ideal Laminate Theory. Note that the scales on the y-axis are different.

To explain this large difference in permeability between oleic and acetic acid, we measured the adsorption of the carboxylic acids to the film surface, as shown in Figure 6.15. We also attempted to measure the solubility of both oleic and acetic acid in LDPE and EAA, but due to their low solubility no reliable results could be obtained. Figure 6.15 shows the results from QCM, where solutions of oleic or acetic acid were flowed over spin-coated films onto a gold surface. The arrows show where injections of acetic and oleic acid in steps of $10\times$ higher concentrations were added. Concentration ranges similar to those used in a permeability experiment are shown within the black circles. Figure 6.15a shows an adsorption of oleic acid to the surfaces of LDPE and EAA in the concentration range used in the permeability experiment. The same adsorption is not seen for acetic acid (Figure 6.15b), and this may be a part of the higher permeability of oleic acid over acetic acid. One could speculate that oleic acid should have higher solubility in LDPE and EAA than acetic acid because of its chemical structure, which also results in a higher permeability according to Equation 14.

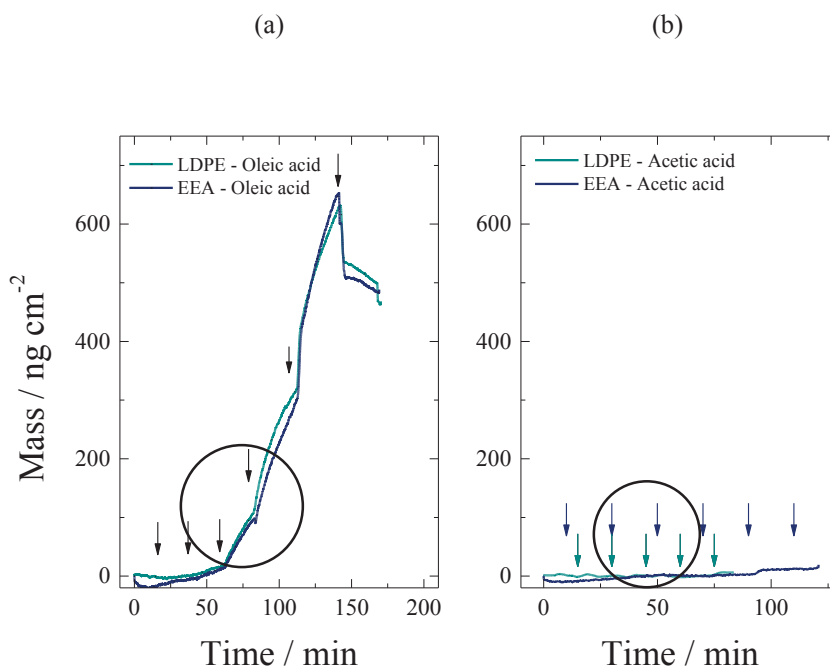


Figure 6.15. QCM results showing (a) adsorption of oleic acid to the LDPE and EAA surface (b) no adsorption of acetic acid. Arrows show when concentrations ranging from $1.2\cdot 10^{-5}$ to $1.2\cdot 10^{-1}$ mg/ml (with an increase in each step by a factor of 10) was added, last arrow shows when the film surface was washed with solvent. Note that the same concentrations was used in (a) and (b) but added at different times.

To discover how the interfaces affected permeability, we used methods such as TOF-SIMS, SAXS, and WAXD to characterize the properties of the interfaces. Using TOF-SIMS, the chemical composition of the film materials could be studied by sputtering with an ion source, which created a crater in the film over time. Figure 6.16 shows the depth profile of the 8-layered film, where the EAA film was placed with the surface closest to the sputter beam. Since EAA has carboxylic groups there should be hydroxyl groups present in the film, and Figure 16.16 presents the intensity of OH- and O-. The intensity goes from 6000 respectively 4000 to almost 0 when reaching the LDPE film. Using the transition time it takes to go from EAA to LDPE, it is possible to calculate an approximate interfacial thickness. In this case, it was calculated to approximately 2 to 2.5 μm .

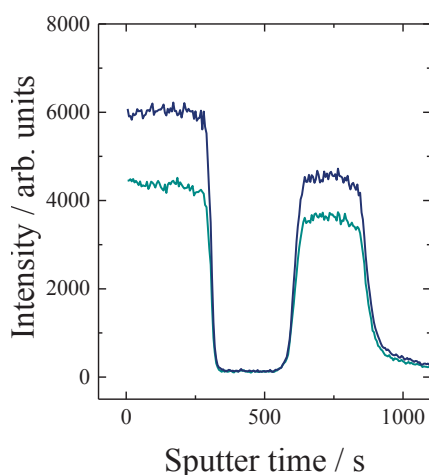


Figure 6.16. Intensity of OH- (blue) and O- (green) in an 8-layered LDPE/EAA film from TOF-SIMS measurement.

Using interfacial thickness, it is possible to calculate *interfacial permeability* using Equation 18. Calculated interfacial permeability is presented in Figure 6.17. The black dots represent the interfacial permeability of oleic acid and show values of 1.2 to $3.8 \cdot 10^{-15} \text{ m}^2/\text{s}$ which is much lower than the permeability measured for the laminates. Similar results are observed for acetic acid, whose interfacial permeability shows values from 0.01 to $0.2 \cdot 10^{-15} \text{ m}^2/\text{s}$. Due to the large differences in permeability

between the laminates and the interfaces, there is reason to believe that there is an additional mechanism acting at the interfaces. One possibility is ordering or induced crystallinity in the interface or close to the interface.

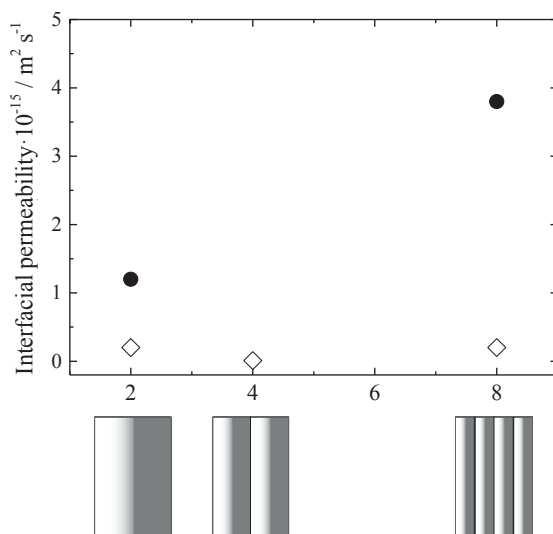


Figure 6.17. Calculated interfacial permeability of oleic acid (●) and acetic acid (◇) for a 2-, 4- and 8-layered film.

To study whether an ordering close to the interface was the reason for lowered permeability, SAXS and WAXD measurements were performed on the LDPE, EAA, and the 2-layered film; results are presented in Table 6.1. Numbers in parenthesis are the theoretical mean values expected for the bulk polymers in the 2-layered film. As seen in the Table, the amorphous-crystalline correlation decreased from 16.2 nm (LDPE) to 12.0 nm (EAA). The theoretical value for the 2-layered film is 13.8 nm, but a value of 14.6 nm was observed. This means that the two layers do interact and form an ordering close to the interface. WAXD measurements showed that the LDPE in the 2-layered film was more ordered than the EAA, which suggests that the co-extrusion of the two films forces an ordering of polymer chains close to the interface. McEvoy and co-workers have shown that transcrystalline layers can form between

Outcome of Research

LDPE and EAA with 3% acrylic acid [55], which could explain these results. Molecular weight and polydispersity was studied using size exclusion chromatography (SEC). The polydispersity was high for both LDPE and EAA, which supports the idea of a transcrystalline layer forming because of shorter chains accumulating in the interface.

Table 6.1. SAXS/WAXD data. Numbers in parenthesis show the theoretical mean values expected for the bulk polymers in LDPE/EAA.

	LDPE	EAA	LDPE/EAA
SAXS			
$\xi(\text{nm})$	16.2	12.0	14.6 (13.8)
WAXD			
$D_{\text{interchain}} (\text{\AA})$	4.12	4.18	4.14 (4.15)

In summary, this study showed that it is possible to decrease the permeability of laminates to less than that of pure films consisting of only one material. This was explained by an ordering of polymer chains close to the interface. Since crystalline parts of a polymer are considered impermeable, total permeability is also expected to decrease with additional layers.

IMPORTANCE OF RESEARCH FOR INDUSTRIAL APPLICATIONS

Composite films of PLA, cellulose, and xyloglucan were produced via extrusion. Increased water permeability was observed in films after the hydrophilic hemicellulose had been adsorbed to the surface of cellulose particles. At the same time an increased storage modulus was observed. These results are important for industry since it seems that the purification of pulp may not be an important step in producing composites with similar mechanical and thermal properties. However, the desired water permeability should of course be taken into consideration when designing the materials. The explanation for the increased storage modulus is the presence of capillary forces between PLA and the hydrophilic xyloglucan. These forces will only be present at low relative humidity, and for materials that require high barrier properties, this is probably not the best solution. However, Xiao and co-workers showed a similar phenomenon for SiO₂ [117], which is not as hydrophilic. Therefore, it could be interesting to test whether the addition of SiO₂ to the surface of cellulose particles (or silica, for example) would result in composites with increased storage modulus and barrier properties.

The surface of CNC was modified with hydrophobic PLA via a ring-opening polymerization. The modified and unmodified nano-fillers were incorporated in different polymers with varying hydrophobicity, where the modified rods dispersed well in the matrices, resulting in more homogenous films. The unmodified rods aggregated and inhomogeneous films formed. Studies of the microstructure and density revealed that pores formed in the films where the well-dispersed modified rod-like nano-fillers were added. These results are mainly important for the understanding and knowledge of pore formation in well-dispersed nano-fillers in a composite and they should be taken into account when producing nanocomposites.

Additionally, we suggest a simple and straightforward method to predict the dispersability of a nano-filler in a matrix by calculating approximate HSP for the filler. These values were compared with known values for solvents and polymers, and we found that it is possible to find a suitable match between polymer matrix and surface-modified fillers. The method can therefore be used to predict the dispersability of a filler in a composite prior to film production, which would save both effort and time.

Importance of Research for Industrial Applications

Last but not least, we show that it is possible to decrease the barrier properties for a laminate compared to a pure polymer film. This is explained by the ordering of chains close to the interface. Combining two materials which in the end creates an ordered structure close to the interface is of course advantageous for the packaging industry where high barrier properties are desired. We believe that the ordering of chains close to the interfaces is a research field that should be more explored.

CONCLUSIONS AND FUTURE OUTLOOK

In order to create functional and efficient barrier, it is important to understand the relationship between structure and the transport properties. Since few material exhibit all properties for a perfect barrier, different materials need to be combined, either as composites or as laminates. In this thesis, the main focus has been to study the mass transport of water in composites and two carboxylic acids in laminates and correlate the barrier properties to the structure of the materials. The major finding is that the mass transport can vary largely depending on the permeant and morphology of the film material.

We have shown that it is possible to control the water permeability to some extent in a biodegradable composite material consisting of PLA and cellulose. This was achieved by the addition of a hydrophilic hemicellulose, which resulted in increased water permeability. At the same time, crystallinity and storage modulus increased. This is interesting for the production of barrier materials and this first study did only cover one ratio of PLA:cellulose while the amount of the hemicellulose was varied. It would be interesting to test further ratios, perhaps another hemicellulose or polymer with higher barrier properties to cover the surface and see if it is possible to also decrease the total permeability.

Furthermore, we have used cellulose nanocrystals as a model system for production of nanocomposites of either PLA, PLGA or LDPE. The surface of cellulose has been modified with different substituents and we have shown that shorter chains (e.g. chains of 6 carbons) are enough to increase the dispersability in a more hydrophobic polymer. However, to increase the adhesion between the filler and the matrix, longer chains need to be attached to the surface of the filler. In this case, chains of 17 carbon chains have been tested, and it would have been interesting to compare both shorter and longer chains and study the dispersability and adhesion in the nanocomposites. Additionally, we observed pore formation in our nanocomposites upon the addition of modified CNC with shorter chains (6 carbons) and suggested a possible mechanism for these pores. Again, it would be interesting to further study the pore formation with other fillers and vary the aspect ratio and substituents on the surface for example.

Another important issue when producing nanocomposites is the dispersability of the nano-filler. Most commonly, the surface of a filler is modified and incorporated in different polymers, where after different properties are studied. This strategy is time-

Conclusions and Future Outlook

consuming and the results are not always the desired. In this project, we made a first trial to predict the dispersability of surface-modified CNC's using solvents with known HSP. The method was validated by an extensive characterization of the produced nanocomposites, but it certainly needs to be further developed and validated using other polymers and fillers.

Last, the use of laminates is common in the packaging industry. We have shown that it is possible the decrease permeability by a factor of four using carboxylic acids rather than pure film materials for laminates. This observation was explained by an ordering of polymer chains close to the interface, which function as a hindrance for the permeants. It would be truly interesting to see whether this is the case for other polymers, permeants, and different gases.

ACKNOWLEDGMENTS

The VINN Excellence Centre SuMo Biomaterials (Supramolecular Biomaterials – Structure, Dynamics and Properties) is gratefully acknowledged for financial support.

I would also like to acknowledge the following people for their contributions to my project:

- First of all, thanks to my supervisors Anette Larsson and Niklas Lorén, who gave me the opportunity to do this PhD project. I have really enjoyed this time and it feels sad that it is over! And Anette, I don't even know how to thank you for all your time and effort during these years! You have believed in me from the start and you have taught me so much, not just about science, but also other important parts of life! You have been a great inspiration and I really like our scientific discussions, even during maternity leave!
- Thanks to Sven Engström for being a great examiner.
- All companies and people involved in SuMo Biomaterials, for valuable advice and discussions and for your interest and contributions to my project. It has been a pleasure being involved in this center. Special thanks to Berit Stålbom and her group at Tetra Pak for letting me occupy your desks while summing up my thesis.
- All my co-authors for interesting discussions and help with the writing. Special thanks to Anna Ström, for valuable discussions about science, but also about life. I am really happy that I got to know you and I hope we will keep in touch in the future! Also, thanks to Romain Bordes for help with equipment and measurements as well as discussions. Thanks to Anna Bergstrand for all your proof-reading and for always having good advice to give!
- The people in my advisory group in SuMo (both former and present). Special thanks to Thorbjörn Andersson, who initiated this PhD project and has been a great inspiration through the whole project! Also, special thanks to Michael Persson, who helped me to take the project one step further by introducing new ideas.
- People in the Pharmaceutical group, both former and present. Special thanks to my former room-mate Anders Johnsson for being a good friend, to Jurgita Kazlauske for always being so happy and helpful, and Johanna for always helping me with different computer related problems. Thanks to Helene Andersson, Hanne Evenbratt and Annika Borde for nice discussions and all time spent on conferences. And Magnus Svensson, for all you help!

Acknowledgments

- All the people, past and present, on “floor 8”, who made and make it such a nice workplace! Especially Anders Lennartsson, Camilla Johansson, Lanlan Sun, Markus Jarvid, Mattias Andersson, Sophia Wassén, and Zandra George for all the nice *fikapaus*.
- My diploma workers: Åsa Hermansson, Camilla Börstell, and Aina Viladot for your contribution to my project. Also, thanks to diploma workers Stefan Naana and Celine van Vooren, who contributed results to one of my projects. It was a pleasure supervising you and I learned a lot as well!
- Thanks to Arne Holmström, Anne Wendel, and Anders Mårtensson for help with science, equipment, and practical issues!
- Thanks to Carina Pettersson, Frida Andersson, Lotta Pettersson, and Ann Jakobsson for all your help with administrative stuff!
- Last, but certainly not least, thanks to my friends and family! Thanks to my parents, who have always supported me and been there for me, no matter what! It is really appreciated! My sister, with whom I have shared the time in academia. Even though we have been on the opposite sides of the earth, our discussions are much appreciated and much needed! And last, thanks to Erik and my daughter Amanda, who are the lights of my life and remind me of what is important!

REFERENCES

-
- [1] E.T.H. Vink, K.R. Rábago, D.A. Glassner, P.R. Gruber, *Polymer Degradation and Stability*, 80 (2003) 403-419.
- [2] K.G. Harding, J.S. Dennis, H. von Blottnitz, S.T.L. Harrison, *Journal of Biotechnology*, 130 (2007) 57-66.
- [3] D.W.v. Krevelen, K.t. Nijenhuis, *Properties of Polymers - Their Correlation with Chemical Structure; Their Numerical Estimation and Prediction from Additive Group Contributions* Elsevier, 2009.
- [4] J. Crank, G. Park, *Diffusion in polymers*, Academic Press, New York, 1968.
- [5] J.M. Lagaron, R. Catalá, R. Gavara, *Materials Science and Technology*, 20 (2004) 1-7.
- [6] L.E. Nielsen, *Journal of Macromolecular Science: Part A - Chemistry*, 1 (1967) 929-942.
- [7] R.K. Bharadwaj, *Macromolecules*, 34 (2001) 9189-9192.
- [8] V. Favier, H. Chanzy, J.Y. Cavaille, *Macromolecules*, 28 (1995) 6365-6367.
- [9] L. Petersson, I. Kvien, K. Oksman, *Composites Science and Technology*, 67 (2007) 2535-2544.
- [10] L. Petersson, K. Oksman, *Composites Science and Technology*, 66 (2006) 2187-2196.
- [11] K. Oksman, M. Skrifvars, J.-F. Selin, *Composites Science and Technology*, 63 (2003) 1317-1324.
- [12] M. Hietala, A.P. Mathew, K. Oksman, *European Polymer Journal*, 49 (2013) 950-956.
- [13] A. Carlmark, E. Larsson, E. Malmström, *European Polymer Journal*, 48 (2012) 1646-1659.
- [14] H. Lönnberg, Q. Zhou, H. Brumer, T.T. Teeri, E. Malmström, A. Hult, *Biomacromolecules*, 7 (2006) 2178-2185.
- [15] G. Raj, E. Balnois, M.-A. Helias, C. Baley, Y. Grohens, *Journal of Materials Science*, 47 (2012) 2175-2181.
- [16] E. Espino-Pérez, J. Bras, V. Ducruet, A. Guinault, A. Dufresne, S. Domenek, *European Polymer Journal*, 49 (2013) 3144-3154.
- [17] B. Bax, J. Müssig, *Composites Science and Technology*, 68 (2008) 1601-1607.
- [18] P. Hook, J. Heimlich, *The Ohio State University*, 2011.
- [19] E.A. Association, *European Aluminium Association*, Brussels, 1997.
- [20] N. Anyadike, *Aluminium: The challenges ahead*, Woodhead Publishing Cambridge, England, 2002.
- [21] J. Gerdeen, R. Ronald, *Engineering Design with Polymers and Composites*, CRC Press, United States of America, 2012.
- [22] U.W. Gedde, *Polymer Physics*, Kluwer Academic Publishers, The Netherlands, 1999.
- [23] C. Vasile, M. Pascu, L. Rapra Technology, *Practical guide to polyethylene*, RAPRA Technology, Shrewsbury, 2005.
- [24] S. Pilla, *Handbook of Bioplastics and Biocomposites Engineering Applications*, Wiley - Scrivener, Salem, Massachusetts, 2011.
- [25] Y. Inoue, N. Yoshie, *Progress in Polymer Science*, 17 (1992) 571-610.
- [26] H. Kawamoto, *Science & Technology trends*, (2007) 62-75.
- [27] G. Kale, R. Auras, S.P. Singh, *Journal of Polymers and the Environment*, 14 (2006) 317-334.
- [28] I. Armentano, M. Dottori, E. Fortunati, S. Mattioli, J.M. Kenny, *Polymer Degradation and Stability*, 95 (2010) 2126-2146.
- [29] L.I.F. Moura, A.M.A. Dias, E. Carvalho, H.C. de Sousa, *Acta Biomaterialia*, 9 (2013) 7093-7114.
- [30] R.A. Auras, B. Harte, S. Selke, R. Hernandez, *Journal of Plastic Film and Sheeting*, 19 (2003) 123-135.

References

- [31] A.P. Mathew, K. Oksman, M. Sain, *Journal of Applied Polymer Science*, 101 (2006) 300-310.
- [32] L. Suryanegara, A.N. Nakagaito, H. Yano, *Composites Science and Technology*, 69 (2009) 1187-1192.
- [33] A.-L. Goffin, J.-M. Raquez, E. Duquesne, G. Siqueira, Y. Habibi, A. Dufresne, P. Dubois, *Biomacromolecules*, 12 (2011) 2456-2465.
- [34] A. Pei, Q. Zhou, L.A. Berglund, *Composites Science and Technology*, 70 (2010) 815-821.
- [35] M.D. Sanchez-Garcia, J.M. Lagaron, *Cellulose*, 17 (2010) 987-1004.
- [36] D. Klemm, F. Kramer, S. Moritz, T. Lindström, M. Ankerfors, D. Gray, A. Dorris, *Angewandte Chemie International Edition*, 50 (2011) 5438-5466.
- [37] K. Hossain, I. Ahmed, A. Parsons, C. Scotchford, G. Walker, W. Thielemans, C. Rudd, *Journal of Materials Science*, 47 (2012) 2675-2686.
- [38] N. Lin, J. Huang, P.R. Chang, J. Feng, J. Yu, *Carbohydrate Polymers*, 83 (2011) 1834-1842.
- [39] M. Pereda, G. Amica, I. Rácz, N. Marcovich, *Journal of Food Engineering*, 103 (2011) 76-83.
- [40] E. Fortunati, I. Armentano, Q. Zhou, A. Iannoni, E. Saino, L. Visai, L.A. Berglund, J.M. Kenny, *Carbohydrate Polymers*, 87 (2012) 1596-1605.
- [41] E. Fortunati, M. Peltzer, I. Armentano, L. Torre, A. Jiménez, J.M. Kenny, *Carbohydrate Polymers*, 90 (2012) 948-956.
- [42] E.L. Cussler, *Diffusion Fundamentals*, 6 (2007) 72.71-72.12.
- [43] A. Turner, *Packaging Technology and Science*, 7 (1994) 99-99.
- [44] A. Peacock, *Handbook of Polyethylene: Structures, Properties and Applications*, Marcel Dekker, New York, 2000.
- [45] J. Schultz, A. Carré, C. Mazeau, *International Journal of Adhesion and Adhesives*, 4 (1984) 163-168.
- [46] L. Ulrén, T. Hjertberg, *Journal of Applied Polymer Science*, 37 (1989) 1269-1285.
- [47] G. Olafsson, M. Jägerstad, R. Öste, B. Wesslén, *Journal of Food Science*, 58 (1993) 215-219.
- [48] C.-M. Wu, M. Chen, J. Karger-Kocsis, *Polymer Bulletin*, 41 (1998) 239-245.
- [49] N. Billon, C. Magnet, J.M. Haudin, D. Lefebvre, *Colloid and Polymer Science*, 272 (1994) 633-654.
- [50] D.R. Fitchmun, S. Newman, *Journal of Polymer Science Part A-2: Polymer Physics*, 8 (1970) 1545-1564.
- [51] S. Mukhopadhyay, B.L. Deopura, R. Alagiruswamy, *Journal of Thermoplastic Composite Materials*, 16 (2003) 479-495.
- [52] N. Klein, G. Marom, A. Pegoretti, C. Migliaresi, *Composites*, 26 (1995) 707-712.
- [53] H. Xu, L. Xie, X. Jiang, X.-J. Li, Y. Li, Z.-J. Zhang, G.-J. Zhong, Z.-M. Li, *The Journal of Physical Chemistry B*, 118 (2013) 812-823.
- [54] D. Broseta, G.H. Fredrickson, E. Helfand, L. Leibler, *Macromolecules*, 23 (1990) 132-139.
- [55] R.L. McEvoy, S. Krause, *Macromolecules*, 29 (1996) 4258-4266.
- [56] P. Wynblatt, *Introduction to interfaces and diffusion*, in: V. Getta (Ed.) *Material issues for generation IV systems*, Springer Science, 2008, pp. 393-423.
- [57] M. Stamm, *Polymer Surface and Interface Characterization Techniques*, *Polymer Surfaces and Interfaces*, Springer, 2008.
- [58] H. Eklind, *Department of Polymer Technology*, Chalmers University of Technology, Göteborg, 1996, pp. 1-42.
- [59] D. McLean, *Grain Boundaries in Metals* Clarendon Press, Oxfordmc, 1957.
- [60] R. Schnell, M. Stamm, *Macromolecules*, 31 (1998) 2284-2292.

References

- [61] M. Doi, S.F. Edwards, *The theory of polymer dynamics*, Clarendon, Oxford, 1986.
- [62] P.G. de Gennes, *The Journal of Chemical Physics*, 55 (1971) 572-579.
- [63] P.W. Busch, R., *Interfaces between incompatible polymers*, *Polymer Surfaces and Interfaces*, 2008.
- [64] H. Wang, K. J.K., A. Hiltner, E. Baer, B. Freeman, A. Rozanski, A. Galeski, *Science*, 323 (2009) 757-760.
- [65] S.H. Anastasiadis, I. Gancarz, J.T. Koberstein, *Macromolecules*, 21 (1988) 2980-2987.
- [66] P.J. Flory, *The Journal of Chemical Physics*, 10 (1942) 51-61.
- [67] M.L. Huggins, *The Journal of Physical Chemistry*, 46 (1942) 151-158.
- [68] M.L. Huggins, *Annals of the New York Academy of Sciences*, 43 (1942) 1-32.
- [69] P.J. Flory, *The Journal of Chemical Physics*, 12 (1944) 425-438.
- [70] B. Guckenbiel, M. Stamm, T. Springer, *Physica B*, 198 (1994) 127-131.
- [71] D.W. Schubert, V. Abetz, M. Stamm, T. Hack, W. Siol, *Macromolecules*, 28 (1995) 2519-2525.
- [72] J. Noolandi, K.M. Hong, *Macromolecules*, 15 (1982) 482-492.
- [73] E.L. Jablonski, Iowa State University, Ames, Iowa, 2002.
- [74] B.K. Fink, R.L. McCullough, *Composites Part A: Applied Science and Manufacturing*, 30 (1999) 1-2.
- [75] D.K. Hale, *Journal of Materials Science*, 11 (1976) 2105-2141.
- [76] S. Gårdebjer, A. Larsson, C. Löfgren, A. Ström, *Journal of Applied Polymer Science*, 132 (2015) n/a-n/a.
- [77] E. Manias, *Journal Nature Materials*, 6 (2007) 9-11.
- [78] F. Du, R.C. Scogna, W. Zhou, S. Brand, J.E. Fischer, K.I. Winey, *Macromolecules*, 37 (2004) 9048-9055.
- [79] L.S. Schadler, *Polymer-Based and Polymer-Filled Nanocomposites*, *Nanocomposite Science and Technology*, Wiley-VCH Verlag GmbH & Co. KGaA, 2004, pp. 77-153.
- [80] S. Gårdebjer, A. Bergstrand, A. Idström, C. Börstell, S. Naana, L. Nordstierna, A. Larsson, *Composites Science and Technology*, 107 (2015) 1-9.
- [81] P. Qu, Y. Zhou, X. Zhang, S. Yao, L. Zhang, *Journal of Applied Polymer Science*, 125 (2012) 3084-3091.
- [82] I. Filpponen, E. Kontturi, S. Nummelin, H. Rosilo, E. Kolehmainen, O. Ikkala, J. Laine, *Biomacromolecules*, 13 (2012) 736-742.
- [83] B. Braun, J.R. Dorgan, L.O. Hollingsworth, *Biomacromolecules*, 13 (2012) 2013-2019.
- [84] S. Fujisawa, T. Saito, S. Kimura, T. Iwata, A. Isogai, *Composites Science and Technology*, 90 (2014) 96-101.
- [85] C. Baley, F. Busnel, Y. Grohens, O. Sire, *Composites Part A: Applied Science and Manufacturing*, 37 (2006) 1626-1637.
- [86] L. Xiao, Y. Mai, F. He, L. Yu, L. Zhang, H. Tang, G. Yang, *Journal of Materials Chemistry*, 22 (2012) 15732-15739.
- [87] S. Hüttenbach, M. Stamm, G. Reiter, M. Foster, *Langmuir*, 7 (1991) 2438-2442.
- [88] U.K. Chaturvedi, U. Steiner, O. Zak, G. Krausch, J. Klein, *Physical Review Letters*, 63 (1989) 616-619.
- [89] D.M. Brewis, D. Briggs, *Polymer*, 22 (1981) 7-16.
- [90] T. Hjertberg, B.Å. Sultan, E.M. Sörvik, *Journal of Applied Polymer Science*, 37 (1989) 1183-1195.
- [91] G. Olafsson, I. Hildingsson, *Journal of Agricultural and Food Chemistry*, 43 (1995) 306-312.
- [92] M.A. Schroeder, B.R. Harte, J.R. Giacini, R.J. Hernandez, *Journal of Plastic Film and Sheeting*, 6 (1990) 232-246.
- [93] G. Ortiz, Á. Garrido-López, M.T. Tena, *Packaging Technology and Science*, 20 (2007) 173-182.

References

- [94] S.D. Bergin, Z. Sun, D. Rickard, P.V. Streich, J.P. Hamilton, J.N. Coleman, *ACS Nano*, 3 (2009) 2340-2350.
- [95] M. Mutz, E. Eastwood, M.D. Dadmun, *The Journal of Physical Chemistry C*, 117 (2013) 13230-13238.
- [96] J. Hildebrand, R.L. Scott, *The solubility of nonelectrolytes*, Reinhold, New York, 1950.
- [97] M. Rubinstein, R.H. Colby, *Polymer Physics*, 1 ed., Oxford University Press, Oxford, 2003.
- [98] C.M. Hansen, *Hansen Solubility Parameters - A User's Handbook*, CRC Press, Boca Raton, FL, 2007.
- [99] T. Graham, *Philosophical Transactions of the Royal Society of London*, 156 (1866) 399-439.
- [100] W.J. Koros, *Barrier Polymers and Structures*, ACS American Chemical Society, Washington, 1990.
- [101] L. Masaro, X.X. Zhu, *Progress in Polymer Science*, 24 (1999) 731-775.
- [102] D. Kim, J.M. Caruthers, N.A. Peppas, *Macromolecules*, 26 (1993) 1841-1847.
- [103] A.R. Berens, H.B. Hopfenberg, *Journal of Membrane Science*, 10 (1982) 283-303.
- [104] N. Yi-Yan, R.M. Felder, W.J. Koros, *Journal of Applied Polymer Science*, 25 (1980) 1755-1774.
- [105] S.C. George, S. Thomas, *Progress in Polymer Science*, 26 (2001) 985-1017.
- [106] V. Siracusa, *International Journal of Polymer Science*, 2012 (2012) 11.
- [107] D.U. Liu, X.W. Yuan, D. Bhattacharyya, A.J. Eastale, *EXPRESS Polymer Letters*, 4 (2010) 26-31.
- [108] S. Gårdebjer, A. Bergstrand, A. Larsson, *European Polymer Journal*, 57 (2014) 160-168.
- [109] M.D. Sanchez-Garcia, E. Gimenez, J.M. Lagaron, *Carbohydrate Polymers*, 71 (2008) 235-244.
- [110] J.-W. Rhim, S.-I. Hong, H.-M. Park, P.K.W. Ng, *Journal of Agricultural and Food Chemistry*, 54 (2006) 5814-5822.
- [111] E. Fortunati, I. Armentano, Q. Zhou, D. Puglia, A. Terenzi, L.A. Berglund, J.M. Kenny, *Polymer Degradation and Stability*, 97 (2012) 2027-2036.
- [112] A. Grüniger, P. Rudolf von Rohr, *Thin Solid Films*, 459 (2004) 308-312.
- [113] V. Stannett, *Permeability of plastic films and coated paper to gases and vapors*, Technical Association of the Pulp and Paper, Industry, New York, 1962.
- [114] K.M. Furuheim, NTNU Department of Chemical Engineering Trondheim, Norway, 2002.
- [115] T. Hayashi, M.P.F. Marsden, D.P. Delmer, *Plant Physiology*, 83 (1987) 384-389.
- [116] A.W. Zykwinska, M.-C.J. Ralet, C.D. Garnier, J.-F.J. Thibault, *Plant Physiology*, 139 (2005) 397-407.
- [117] X. Xiao, L. Qian, *Langmuir*, 16 (2000) 8153-8158.
- [118] R.J. Moon, A. Martini, J. Nairn, J. Simonsen, J. Youngblood, *Chemical Society Reviews*, 40 (2011) 3941-3994.
- [119] A.M. Wierenga, A.P. Philipse, *Colloids and Surfaces A: Physicochemical and Engineering Aspects*, 137 (1998) 355-372.
- [120] M. Bercea, P. Navard, *Macromolecules*, 33 (2000) 6011-6016.
- [121] P. Keblinski, J.A. Eastman, D.G. Cahill, *Materials Today*, 8 (2005) 36-44.
- [122] C. Haisheng, D. Yulong, T. Chunqing, *New Journal of Physics*, 9 (2007) 367.
- [123] G.R. Vakili-Nezhaad, A. Dorany, *Chemical Engineering Communications*, 196 (2009) 997-1007.

**Controlling water permeability of biodegradable composite films of polylactide acid,
cellulose and xyloglucan**

Sofie Gårdebjerg, Anette Larsson, Caroline Löfgren, Anna Ström

Journal of Applied Polymer Science 2015, 132, 41219

**Solid-state NMR to quantify surface coverage and chain length of lactic acid modified
cellulose nanocrystals, used as filler in biodegradable composites**

Sofie Gårdebjer, Anna Bergstrand, Alexander Idström, Camilla Börstell, Stefan
Naana, Lars Nordstierna, Anette Larsson

Composite Science and Technology 2015, 107, 1-9

A mechanistic approach to explain the relation between increased dispersion of surface modified cellulose nanocrystals and final porosity in biodegradable films

Sofie Gårdebjer, Anna Bergstrand, Anette Larsson

European Polymer Journal 2014, 57, 160-168

**Using Hansen Solubility Parameters to predict dispersion of nano-particles in polymeric
films**

Sofie Gårdebjer, Martin Andersson, Jonas Engström, Per Restorp, Michael
Persson, Anette Larsson

Accepted in Polymer Chemistry, 2016

The impact of interfaces in laminates for transport of carboxylic acids

Sofie Gårdebjer, Tobias Gebäck, Thorbjörn Andersson, Emiliano Fratini, Piero Baglioni,
Romain Bordes, Anna Viridén, Mark Nicholas, Niklas Lorén, Anette Larsson

Submitted

